

Annual Report
MOU #AM10560 NYSDEC & SUNY Stony Brook
For the period January 1, 2021 – December 31, 2021
New York State Environmental Protection Fund Ocean and Great Lakes Program, NYSDEC

December 31, 2021

The MOU titled, "Development and implementation of an ocean ecosystem monitoring program for New York Bight" between the New York State Department of Environmental Conservation (NYS DEC) and the School of Marine and Atmospheric Sciences (SoMAS) at Stony Brook University is to develop an interdisciplinary, multi-trophic level-ocean monitoring program in the New York Bight in order to provide information on the status of New York pelagic resources to managers; and to inform the development of a system of indicators of ecosystem health using existing data and observations collected in the coastal and offshore monitoring program in order to better inform decision making regionally and locally. This report follows the categories of activities found in the scope of work in that MOU.

Contact Lead Principal Investigator Lesley Thorne with questions or comments.
lesley.thorne@stonybrook.edu

Principal Investigators: Lesley Thorne, Associate Professor; Janet Nye, Associate Professor; Joe Warren, Associate Professor; Charlie Flagg, Research Professor

Report Contributors: Eleanor Heywood, Cetacean and Seabird Technician; Tyler Menz, Carbonate Chemistry Technician; Toniann Keiling, Oceanography Technician; Hannah Blair, PhD Student; Rachel Carlowicz, MS student; Brandyn Lucca, PhD Student; Julia Stepanuk, PhD Student; Nathan Hirtle, PhD Student; Mark Wiggins, Operational Facilities Manager; Tom Wilson, Instrument Laboratory; Baoshan Chen, Carbonate Chemistry Research Associate; Laura Gruenburg, Postdoctoral Research Scientist

TABLE OF CONTENTS

SUMMARY OF ACCOMPLISHMENTS	6
OBJECTIVE 1: EXAMINATION OF AVAILABLE DATA AND IDENTIFYING DATA GAPS.	10
OBJECTIVE 2: MONITOR THE PHYSICAL ENVIRONMENT INCLUDING TEMPERATURE, SALINITY, FLUORESCENCE, AND CARBONATE CHEMISTRY	11
2.1: SHIPBOARD MEASUREMENTS OF PHYSICAL WATER PROPERTIES	11
2.2: CARBONATE CHEMISTRY	14
2.3: GLIDER OPERATIONS	21
OBJECTIVE 3: CHARACTERIZE LOWER TROPHIC LEVEL PRODUCTIVITY	25
OBJECTIVE 4: QUANTIFY ABUNDANCE AND DISTRIBUTION OF PELAGIC FISHES AND SQUID IN THE NEW YORK BIGHT	31
OBJECTIVE 5: COLLECT OPPORTUNISTIC SIGHTING AND BEHAVIORAL DATA OF CETACEANS IN THE NEW YORK BIGHT	34
5.1 SEABIRD AND MARINE MAMMAL LINE-TRANSECT SURVEYS.....	34
5.2 UAV SURVEYS OF HUMPBACK WHALES AND ONGOING BODY VOLUME AND BODY CONDITION ANALYSES.....	34
OBJECTIVE 6: CHARACTERIZE TROPHIC INTERACTIONS AND OCEANOGRAPHIC DRIVERS OF LIVING MARINE RESOURCES	40
OBJECTIVE 7: PROVIDE SUPPLEMENTAL R/V SEAWOLF VESSEL STAFFING SUPPORT	41
OBJECTIVE 8: ISSUES ENCOUNTERED DURING THIS PERIOD	41
WORK PLANNED FOR UPCOMING QUARTERS:	42
REFERENCES	44

List of Figures

FIGURE 1. GENERAL CRUISE MAP, DISPLAYING ASSIGNED STATION NUMBERS AND LOCATIONS FOR SURVEY TRANSECTS (NUMBERED 1-7 AS INDICATED ON STATION NUMBERS).	8
FIGURE 2. FISHERIES ACOUSTIC SURVEY EFFORT (BLACK) AND LOCATIONS OF SAMPLING EFFORTS (RED: LINE-TRANSECT SURVEY EFFORT; GREEN: CTD LOCATIONS; PURPLE: RING NET TOW LOCATIONS; YELLOW: TRAWLING LOCATIONS) FOR ALL OFFSHORE MONITORING CRUISES COMPLETED IN 2021. TWO CTD STATIONS IN THE LONG ISLAND SOUND THAT WERE COMPLETED JUST PRIOR TO THE MAY CRUISE ARE NOT SHOWN HERE BUT ARE INCLUDED IN THE CTD CAST COUNT IN TABLE 1. NOTE THAT NO LONE-TRANSECT SURVEYS OR FISH TRAWLS WERE CONDUCTED DURING EITHER MONITORING CRUISE.	9
FIGURE 3. TEMPERATURE CONTOURS OF CTD CASTS TAKEN ON TRANSECT 6 TO ILLUSTRATE SEASONAL AND INTERANNUAL VARIABILITY IN THE MID-ATLANTIC COLD POOL, WHICH IS DEFINED AS BOTTOM WATER <10°C (PURPLE COLORS). TRANSECT NUMBERS ARE LABELED IN FIGURE 1 FOR REFERENCE.	12
FIGURE 4. TEMPERATURE AT TRANSECT 1 (RIGHT) AND TRANSECT 6 (LEFT) ON THE FOUR 2019 CRUISES. BLANK SPACES INDICATE THAT TRANSECT WAS NOT SAMPLED. THE MID-ATLANTIC COLD POOL IS DEFINED HERE AS BOTTOM WATER <10°C (PURPLE COLORS). TRANSECT NUMBERS ARE LABELED IN FIGURE 1 FOR REFERENCE.	13
FIGURE 5. SEASONAL MAPS OF SURFACE WATER PCO ₂ , AN INDICATOR OF THE ABILITY OF THE OCEAN TO ABSORB CO ₂ FROM OR RELEASE CO ₂ TO THE ATMOSPHERE. ATMOSPHERIC PCO ₂ LEVEL IS ~ 400 MATM, WARM COLORS INDICATE THE OCEAN IS DEGASSING CO ₂ TO THE ATMOSPHERE.	16
FIGURE 6. RELATIONSHIP OF TOTAL ALKALINITY (TA) AND SALINITY FOR DISCRETE SAMPLES COLLECTED IN THE SIX NYOS OFFSHORE CRUISES.	17
FIGURE 7. SEASONAL BOTTOM ARAGONITE SATURATION STATE FROM 2019 CRUISES. THE CONTOURED AREAS INDICATE REGIONS WHERE THE SATURATION STATE IS UNDER 1.5.	18
FIGURE 8. ARAGONITE SATURATION STATE THROUGHOUT THE WATER COLUMN AT EACH TRANSECT FROM NYOS1910. TRANSECT 2 (T2) CAN BE SEEN ON THE LEFT SIDE OF THE MAP AND TRANSECT 1 IS ON THE RIGHT. THE AREA UNDER THE CONTOURS REPRESENTS AREAS WHERE THE SATURATION IS LESS THAN 1.5. TRANSECT NUMBERS ARE LABELED IN FIGURE 1 FOR REFERENCE.	19
FIGURE 9. ARAGONITE SATURATION STATE THROUGHOUT THE WATER COLUMN AT EACH TRANSECT FROM NYOS1907. TRANSECT 6 CAN BE SEEN IN THE BOTTOM LEFT PANEL AND IS INDICATED BY THE LINE OF DOTS NEXT TO T6. TRANSECT NUMBERS DECREASE GOING EAST TO TRANSECT 1 (T1). TRANSECT NUMBERS ARE LABELED IN FIGURE 1 FOR REFERENCE.	20
FIGURE 10. SBU01 GLIDER TRACK LINES FOR ALL SIX DEPLOYMENTS IN THE NEW YORK BIGHT.	21
FIGURE 11. ALONG-TRACK SALINITY, TEMPERATURE, AND DENSITY PLOTS FROM THE FALL 2021 DEPLOYMENT, SBU01_06.	22
FIGURE 12. ALONG-TRACK CHLOROPHYLL, DISSOLVE OXYGEN SATURATION (%), AND pH PLOTS FROM THE FALL 2021 DEPLOYMENT, SBU01_06.	23
FIGURE 13. SUPERPOSITION OF THE TEMPERATURE/SALINITY DIAGRAMS FROM ALL SIX DEPLOYMENTS SHOWING THE RANGE OF PROPERTIES EXPERIENCED BY THE WATERS OF THE NEW YORK BIGHT. THE SEASONAL DEPLOYMENTS COVERED WINTER (SBU01_3), SPRING (SBU01_4), SUMMER (SBU01_1,SBU01_5), AND FALL (SBU01_2, SBU01_6).	24
FIGURE 14. COMMON ZOOPLANKTON COLLECTED IN VERTICAL NET TOWS DURING THE NY OFFSHORE INDICATORS CRUISES. IDENTIFICATIONS FROM LEFT TO RIGHT ARE: RED CYCLOPOID ONCAEA SP., ECHINODERM LARVAE, COPEPOD CENTROPAGES BRADYII, PTEROPOD HYALOCYLIS STRIATA, AND HARPACTICOID MIRACIA EFFERATA. BLACK LINES ON THE RULERS BEHIND THE ANIMALS IN THE IMAGES MARK 1 MM MEASUREMENTS.	25

FIGURE 15. SPATIAL DISTRIBUTIONS OF ALL CLADOCERAN SPECIES FOR EACH OF THE 2020 CRUISES, IN FEBRUARY, JUNE, AND OCTOBER 2020. THE FULL SURVEY GRID INCLUDES 39 STATIONS (OPEN GRAY SQUARES), BUT DUE TO CRUISE CONDITIONS, NET TOW SAMPLING WAS ONLY CONDUCTED AT SOME STATIONS (OPEN ORANGE SQUARES), AND DUE TO LONG PROCESSING TIMES, A SUBSAMPLE OF COLLECTED SAMPLES WAS PROCESSED (FILLED ORANGE DIAMONDS). THE BLACK CIRCLES SHOW THE RELATIVE DENSITIES OF CLADOCERANS AT SITES WHERE THEY WERE PRESENT. CLADOCERANS WERE MOST ABUNDANT IN JUNE. HOWEVER, ONLY SAMPLES FROM INSHORE STATIONS WERE COLLECTED AND PROCESSED..... 26

FIGURE 16. SPATIAL DISTRIBUTIONS OF TWO OF THE MOST ABUNDANT COPEPOD SPECIES FROM THE MAY 2019 CRUISE, CENTROPAGES TYPICUS AND CALANUS FINMARCHICUS. THE FULL SURVEY GRID INCLUDES 39 STATIONS (OPEN GRAY SQUARES), BUT DUE TO CRUISE CONDITIONS, NET TOW SAMPLING WAS ONLY CONDUCTED AND PROCESSED FOR SOME STATIONS (FILLED ORANGE DIAMONDS). THE BLACK CIRCLES SHOW THE RELATIVE DENSITIES OF COPEPOD SPECIES AT SITES WHERE THEY WERE PRESENT. CENTROPAGES TYPICUS DENSITIES WERE HIGHER AT INSHORE STATIONS COMPARED TO CALANUS FINMARCHICUS, WHICH DOMINATED OFFSHORE STATIONS..... 27

FIGURE 17. IMAGES PRODUCED FROM THE ZOO SCAN SYSTEM FROM MULTIPLE 2020 CRUISES. ANIMALS FROM LEFT TO RIGHT ARE: CYCLOPOID ONCAEA SP., ECHINODERM LARVAE, COPEPOD CENTROPAGES BRADYII, PTEROPOD FROM SUBFAMILY CAVALINIINAE, AND HARPACTICOID MICROSETELLA NORVEGICA. SCALE BARS IN EACH IMAGE REPRESENT 1 MM..... 28

FIGURE 18. LIPID RATIOS VARIED BETWEEN 0 AND 69% FOR 30 COPEPODS MEASURED AT EACH STATION DURING THE MAY 2019 CRUISE. THE HIGHEST VARIABILITY IN CALANUS FINMARCHICUS LIPID RATIO CAN BE SEEN AT STATIONS 4.1 AND 6.1.5. THE LIPID RATIO WAS LOWER AT STATION 4.6 COMPARED TO 5.6 AND 6.5. TRANSECT NUMBERS ARE LABELED IN FIGURE 1 FOR SPATIAL REFERENCE. 29

FIGURE 19. PROSOME LENGTHS OF CALANUS FINMARCHICUS WERE SMALLEST (BUT MOST VARIABLE) IN THE FALL COMPARED TO ALL OTHER SEASONS. FOUR WINTER, NINE SPRING, SEVEN SUMMER, AND TWO FALL STATIONS WERE INCLUDED IN THIS DATA SET AND EACH STATION HAD 30 MEASURED COPEPODS REPRESENTING IT. 30

FIGURE 20. AN ECHOGRAM AT 70 KHZ FROM THE MAY 2021 (NYOS2105) CRUISE SHOWED THE PRESENCE OF WEAKLY SCATTERING AGGREGATIONS THAT LIKELY REPRESENT SMALL FISH, SQUID, AND CRUSTACEAN ZOOPLANKTON. THESE DATA WERE COLLECTED FROM TRANSECT 01 AT DEPTHS LESS THAN 100 M. THE BLACK LINE REPRESENTS THE SEAFLOOR. POINT COLOR REPRESENTS S_v (dB RE. 1M^{-1}), WHICH IS THE INTEGRATED, VOLUMETRIC BACKSCATTER FOR THAT PART OF THE WATER COLUMN. 32

FIGURE 21. FISHERY ACOUSTIC SURVEYS PRODUCE SPATIAL MAPS OF NASC ($\text{M}^2 \text{NMI}^{-2}$). HERE EACH PANEL REPRESENTS NASC FOR A DIFFERENT FREQUENCY MEASURED DURING THE MAY 2021 CRUISE. THE COLOR AND SIZE OF EACH CIRCLE ARE SCALED TO HOW MUCH BACKSCATTER OCCURRED AT THAT LOCATION. FOR MANY SPECIES OF INTEREST, NASC WILL BE PROPORTIONAL TO ANIMAL BIOMASS WITH LOWER FREQUENCIES (38 AND 70 KHZ, TOP PANELS) MEASURING SWIMBLADDERED FISH AND SQUID, WHILE HIGHER FREQUENCIES (120 AND 200 KHZ, BOTTOM PANELS) MEASURING SWIMBLADDERLESS FISH AND/OR ZOOPLANKTON. THESE MAPS CAN BE USED TO IDENTIFY AREAS WHERE PELAGIC FISH AND ZOOPLANKTON REGULARLY OCCUR, WHICH CAN BE USEFUL FOR MARINE PLANNING PURPOSES..... 32

FIGURE 22. SEASONAL TRENDS IN NASC ($\text{M}^2 \text{NMI}^{-2}$) WERE TESTED USING THE STRATIFIED MEANS (CROSSED-BOXES) AND 95% CONFIDENCE INTERVALS (LINES) AT EACH FREQUENCY USING AN ALGORITHM ADAPTED FROM JOLLY AND HAMPTON (1990). THE BACKGROUND COLORS REPRESENT SPRING (GREEN), S SUMMER (YELLOW), FALL (ORANGE), AND WINTER (BLUE). THE HORIZONTAL DASHED LINES REPRESENT THE STRATIFIED MEAN NASC AND 95% CONFIDENCE INTERVALS FOR EACH FREQUENCY. NOTE THAT THE Y-AXES AT EACH FREQUENCY ARE NOT THE SAME SINCE NASC VALUES ARE NOT DIRECTLY COMPARABLE ACROSS FREQUENCIES. THESE SUMMARY STATISTICS CAN BE USED TO VIEW BROAD SEASONAL TRENDS IN BACKSCATTER AT EACH FREQUENCY. 33

FIGURE 23. EXAMPLE OF AERIAL IMAGERY OF HUMPBACK WHALES OBTAINED DURING THE 2021 FIELD SEASON. 35

FIGURE 24. SMALL-BOAT UAV SURVEY EFFORT (DARK GREY) AND HUMPBACK WHALE (MEGAPTERA NOVAEANGLIAE) SIGHTINGS (ORANGE) DURING THE 2021 FIELD SEASON. ALL HUMPBACKS FOR WHICH WE WERE ABLE TO CAPTURE AERIAL IMAGERY OCCURRED INSHORE AND DERIVED LENGTHS SUGGEST THEY WERE JUVENILES. IN CONTRAST TO PREVIOUS YEARS, WE ONLY OBSERVED TWO HUMPBACK WHALES IN OFFSHORE WATERS, BUT CONDITIONS PREVENTED THE CREW FROM TRACKING THESE ANIMALS LONG ENOUGH TO OBTAIN AERIAL FOOTAGE. ALL SURVEYS WERE CONDUCTED FROM R/V PARKER. 37
 FIGURE 25. A. EXAMPLE OF A STILL IMAGE CAPTURED FROM UAV AERIAL IMAGE OF A HUMPBACK WHALE SHOWING WIDTH MEASUREMENTS TAKEN AT 5% INTERVALS OF BODY LENGTH. B. THESE MEASUREMENTS ARE THEN USED AS INPUTS TO SCALE 3D MODELS AND OBTAIN VOLUMETRIC ESTIMATES OF HUMPBACK WHALES. 39

List of Tables

TABLE 1. SUMMARY OF SAMPLING EFFORT PER CRUISE. FOR EACH CRUISE THE NUMBER OF RING NET TOWS, CTD CASTS, WATER SAMPLES, AND DAILY SURFACE SEAWATER SAMPLES, AND KILOMETERS OF ACOUSTIC TRANSECT EFFORT ARE DETAILED. ABSENT FOR THIS YEAR’S REPORT ARE LINE-TRANSECT SURVEY EFFORT AND FISH TRAWLS DUE TO OUR PANDEMIC OPERATIONS (REDUCED CREW AND REDUCED OBJECTIVE CRUISES). 7
 TABLE 2. STATUS OF THE 42 INDICATORS OF NEW YORK BIGHT MARINE ECOSYSTEM HEALTH. LETTERS REFER TO INDICATOR STATUS IN EACH YEAR, C=COMPLETED, P=PROPOSED, U=UNDER DEVELOPMENT, R=REFINED. 10
 TABLE 3. TOTAL NUMBER OF SAMPLES COLLECTED AND ANALYZED TO DATE. CRUISES DENOTED WITH * WERE ANALYZED AT THE NOAA LAB IN MILFORD, CT. 14
 TABLE 4. SUMMARY OF UAV SURVEY EFFORT (TIME AND DISTANCE SURVEYED), THE NUMBER OF HUMPBACK WHALES (MEGAPTERA NOVAEANGLIAE) OBSERVED, AND THE NUMBER OF WHALES FOR WHICH WE WERE ABLE TO OBTAIN BODY LENGTH AND BODY VOLUME MEASUREMENTS, RESPECTIVELY. OFFSHORE EFFORT REFERS TO EFFORT THAT PRIMARILY OCCURRED MORE THAN 20 KM FROM SHORE BASED ON OBSERVATIONS OF INSHORE / OFFSHORE AGE-BASED PARTITIONING OF JUVENILES AND ADULT HUMPBACKS IN STEPANUK ET AL. 2021 * INDICATES ONE INDIVIDUAL WAS RESIGHTED (ONCE ON BOTH JULY 20 AND AUGUST 3, 2021 AND ONCE ON JULY 20, 202 * INDICATES ONE INDIVIDUAL WAS RESIGHTED (ONCE ON BOTH JULY 20 AND AUGUST 3, 2021 AND ONCE ON JULY 20, 2021 AND AUGUST 25, 2021. 36
 TABLE 5. ACTIVITIES AND DELIVERABLES FOR UPCOMING QUARTERS. 42

Summary of Accomplishments

This report covers the time period of January 1, 2021-December 31, 2021. We conducted two seasonal shipboard monitoring cruises in March 2021 and May 2021 aboard the R/V Seawolf to monitor the pelagic ecosystem of the New York Bight (NYB) (Table 1; Figure 2). During these cruises we completed 68 CTD stations (including 382 CTD water samples), 126 zooplankton tows (63 station visits), and 3102 km of fish acoustic surveys. Due to the ongoing pandemic and the reduced operations nature of our monitoring cruises, we were unable to safely staff research cruises with enough personnel to conduct midwater fish trawls or conduct line-transect surveys. Our efforts during this period included: (1) the hiring and arrival of our carbonate chemistry research associate, Baoshan Chen, who conducted many tests and troubleshooting of the software and individual equipment components on the VINDTA system in order to ensure the highest precision and accuracy in our analysis of Dissolved Inorganic Carbon (DIC) and total alkalinity (TA). To date, all samples collected on cruises in 2018, 2019, and a majority of those collected in 2020, have been analyzed and processed with quality assurance protocols. (2) designing a new seabird line-transect protocol to be implemented in 2022. (3) Hiring technician, Toniann Keiling, who specializes in fisheries acoustics and zooplankton data collection and processing. (4) Implementing a protocol to identify ichthyoplankton (fish larvae and fish eggs) to species to allow us to assess the distribution and abundance of early life stages of important fishes in the New York Bight. (5) setting up a new zooplankton identification tool to streamline sample processing. (6) Finalizing a 3D model of humpback whales designed to integrate width and length measurements from aerial images in order to generate estimates of body volume. (7) Conducting 2249 km (114.6 hours) of UAV survey effort on the R/V Parker and assessing body condition in 59 humpback whales for which morphometric measurements have been conducted to date. With the continuation of the winter and spring seasonal cruises, we maintained monitoring efforts in the New York Bight and more broadly in the Northeast US, despite vessel maintenance setbacks and a greatly reduced science crew during cruises due to the ongoing SARS-CoV-2 pandemic. A total of 656 water samples were analyzed for DIC and TA. Ongoing collaboration and coordination with other glider operators in the area has increased the data coverage of the Mid-Atlantic and broader Northeast US. Within these varied aspects of the program, we have developed and standardized protocols and have trained field staff to collect samples and perform surveys for multiple objectives. We continued to implement our Data Management plan to store and share data with the New York State Department of Environmental Conservation and to ensure the highest quality control standards for data as it is processed and analyzed. We published two papers from this work in 2021, *Age-specific behavior and habitat use in humpback whales: Implications for vessel strike* in Marine Ecology Progress Series, and *Marine ecosystem indicators are sensitive to ecosystem boundaries and spatial scale* in Ecological Indicators, and a third, *Integrating 3D models with morphometric measurements to improve volumetric estimates in large mammals*, is in review in Methods in Ecology and Evolution. Finally, our new postdoc, Laura Gruenburg, continues to accumulate, analyze and develop new indicators of ocean health. A separate report on these analyses is provided, but a

brief summary is provided below. The continuation of the offshore monitoring program represents the bulk of work covered in this report (Objectives 2-5).

Table 1. Summary of sampling effort per cruise. For each cruise the number of ring net tows, CTD casts, water samples, and daily surface seawater samples, and kilometers of acoustic transect effort are detailed. Absent for this year's report are line-transect survey effort and fish trawls due to our pandemic operations (reduced crew and reduced objective cruises).

Cruise	Dates	Ring-net Tows	CTD Casts	No. Discrete Water Samples	No. Surface Water OA Samples	Fish Acoustic Effort (km)
March 2021	20Mar2021 - 25Mar2021	48	26	136	6	1,267
May 2021	20May2021 - 02Jun2021	78	42	246	10	1,835

Stony Brook University, Stony Brook, NY 11794-5000
 Tel: 631-632-3187; Fax: 631-632-8820

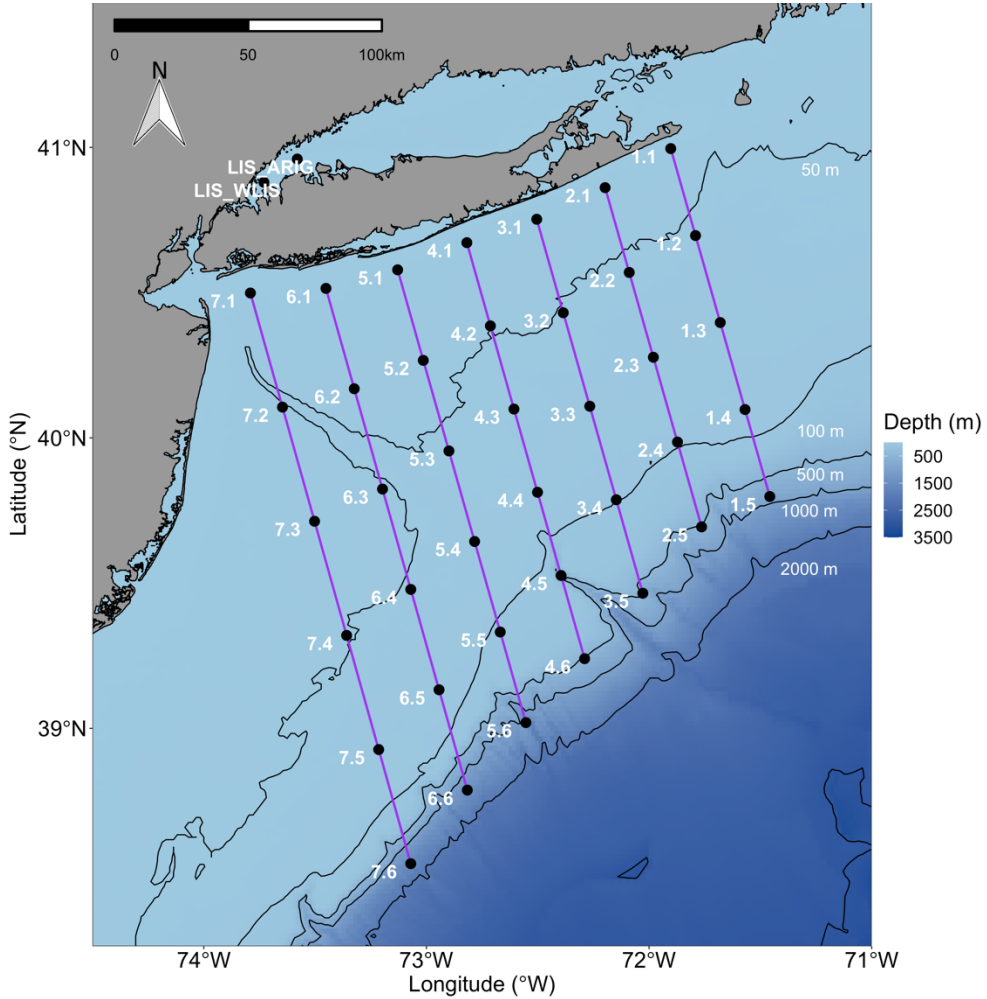


Figure 1. General cruise map, displaying assigned station numbers and locations for survey transects (numbered 1-7 as indicated on station numbers).

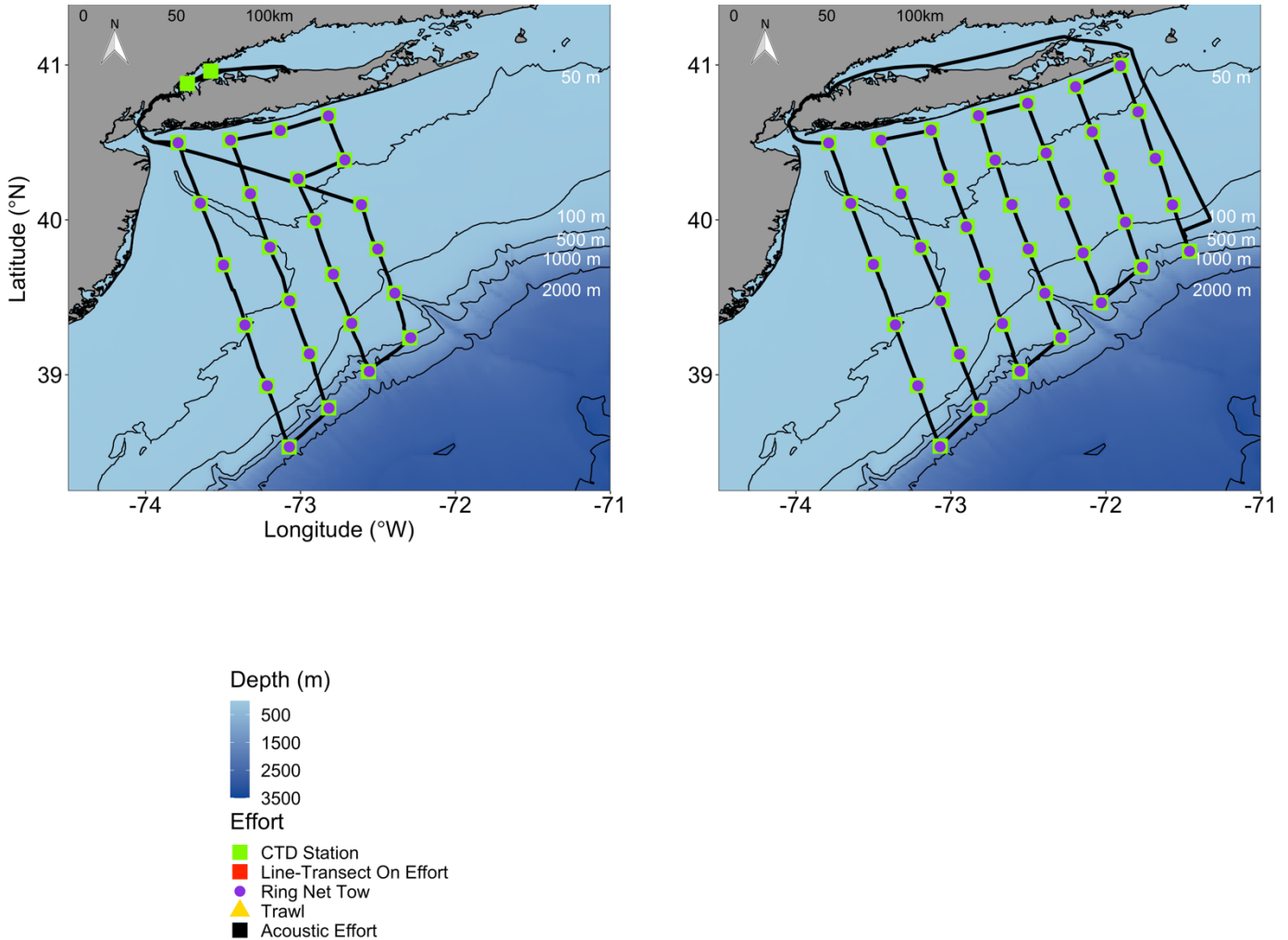


Figure 2. Fisheries acoustic survey effort (black) and locations of sampling efforts (red: line-transect survey effort; green: CTD locations; purple: ring net tow locations; yellow: trawling locations) for all offshore monitoring cruises completed in 2021. Two CTD stations in the Long Island Sound that were completed just prior to the May cruise are not shown here but are included in the CTD cast count in Table 1. Note that no lone-transect surveys or fish trawls were conducted during either monitoring cruise.

Objective 1: Examination of available data and identifying data gaps

In late 2020, 42 indicators were selected by SOMAS and NYSDEC scientists and managers to monitor the health of the NYB (Table 2). Of those, 25 were completed, 15 new indicators were proposed and 3 were already in development. A strategy for the 3 indicators under development for pH, dissolved oxygen, and humpback whale condition has been developed, but only a few years of data exist for each of these. Trends over time in these indicators can be examined with further monitoring. Of the 15 new indicators proposed, all have been developed and we were able to examine trends over time. As indicated in Table 2, many indicators were re-evaluated and refined slightly, and we will similarly refine and vet indicators each year.

Table 2. Status of the 42 indicators of New York Bight marine ecosystem health. Letters refer to indicator status in each year, C=Completed, P=Proposed, U=Under development, R=Refined

Key Ecosystem Component	Indicator	2021 Status	2022 Status
ENVIRONMENT			
Surface Water Temperature	1. Seasonal mean sea surface temperature	C	C
	2. Marine heatwave days	C	C
Water Column Temperature	3. Bottom temperature anomaly	C	C
	4. Cold pool volume	P	C
	5. Cold pool duration	P	U
Water Chemistry	6. Bottom dissolved oxygen	U	C
	7. Subsurface pH, pCO ₂ , aragonite	U	C
Winds	8. Mean wind stress	P	C
	9. Number of large storms	P	U
Stratification	10. Stratification anomaly	C	R, C
Freshwater Inputs	11. Hudson River flow	C	C
Salinity	12. Surface water salinity	C	C
	13. Bottom water salinity	C	C
Climate Variability	14. Global carbon dioxide	C	C
Habitat	15. Lobster thermal habitat	P	C
	16. Location of 20 C isotherm	P	C
MARINE COMMUNITY			
Phytoplankton	17. Monthly mean surface chlorophyll	C	R, C
Zooplankton	18. <i>Calanus finmarchicus</i> abundance	C	C
	19. <i>Centropages typicus</i> abundance	C	C
	20. Small/Large copepod index	C	C
	21. Longfin squid biomass	C	C
Forage Species	22. Northern shortfin squid biomass	C	C
	23. Forage biomass	C	C
Mid-Trophic Level Species	24. NOAA foraging groups	C	C

	25. Total trawl biomass	C	C
	26. Black sea bass biomass	C	C
	27. Summer flounder biomass	C	C
	28. American lobster biomass	P	C
	29. Jonah crab biomass	P	C
	30. Northern vs. summer species biomass	P	C
	31. Structure oriented species	P	C
Upper-Trophic Level Species	32. Humpback whale body condition	U	U
Biodiversity	33. Species richness	P	C
Trophic Interactions	34. Average trophic level of fish community	P	C
	35. Temperature preference of fish community	P	C
HUMAN COMMUNITIES			
Recreational Fishing	36. Recreational harvest (total= harvest + released)	C	C
	37. Recreational effort (number trips)	P	C
Commercial Fishing	38. Commercial fisheries landings (weight)	C	C
	39. Commercial landings value (USD)	C	C
Coastal Communities	40. Human population of Long Island	C	C
	41. Vessel density and speed	P	U
	42. Sea level rise risk for Long Island	C	C

Objective 2: Monitor the physical environment including temperature, salinity, fluorescence, and carbonate chemistry

2.1: Shipboard Measurements of Physical Water Properties

Unfortunately, due to maintenance issues with the R/V Seawolf, we were unable to perform a full survey in the summer and fall of 2021. However, this did allow us time to run a backlog of samples that we were unable to run during COVID and allowed us to focus on quality assurance and control checks on data collected by the underway system on the R/V Seawolf during each cruise. We have continued our comparisons of physiochemical patterns using CTD data collected on each cruise. The Mid-Atlantic cold pool continues to be an oceanographic feature of great importance and is characterized by bottom water <10°C and salinities less than 34 psu. It is an important summer habitat for cold water fishes and invertebrates. Comparison of seasonal cross sections of temperature constructed from CTD casts across transect 6, which was sampled in most cruises illustrate the seasonal and interannual variability in the Mid-Atlantic cold pool and helps inform timing of future cruises (Figure 3). The stratification present in May indicates the development of the cold pool which was not evident in the March cruise. Comparison of the May 2019 and May 2021 shows that the overall size of the cold pool when it is first formed is not too dissimilar, but the water within the cold pool area is slightly higher in 2019 than in 2021 as indicated by the much larger area within the 8°C isotherm in 2021. A similar seasonal trend is

seen in Figure 4 where cross sections of temperature at the easternmost (transect 1) and a more western transect (transect 6) portion of our survey are plotted for the 2019 cruises (Figure 1). Again, there is no evidence of the cold pool present in February, but by May the stratification of the water column shows an area of cold water underneath the warmer surface waters. This area is still present in July when surface waters have warmed even more. However, the size of the cold pool and temperature within the cold pool is different in transect 6 as compared to transect 1, emphasizing the importance of getting good east-west coverage to characterize the entire cold pool area in the NYB. By October, the Mid-Atlantic cold pool is extremely small, if at all present. This seasonal progression is similar to what we found developing an indicator for the Mid-Atlantic cold pool with model output of bottom temperature produced at a much finer spatial scale than our data collection and over many years. The Mid-Atlantic cold pool is rarely present in April and in the last decade has not been detected in October.

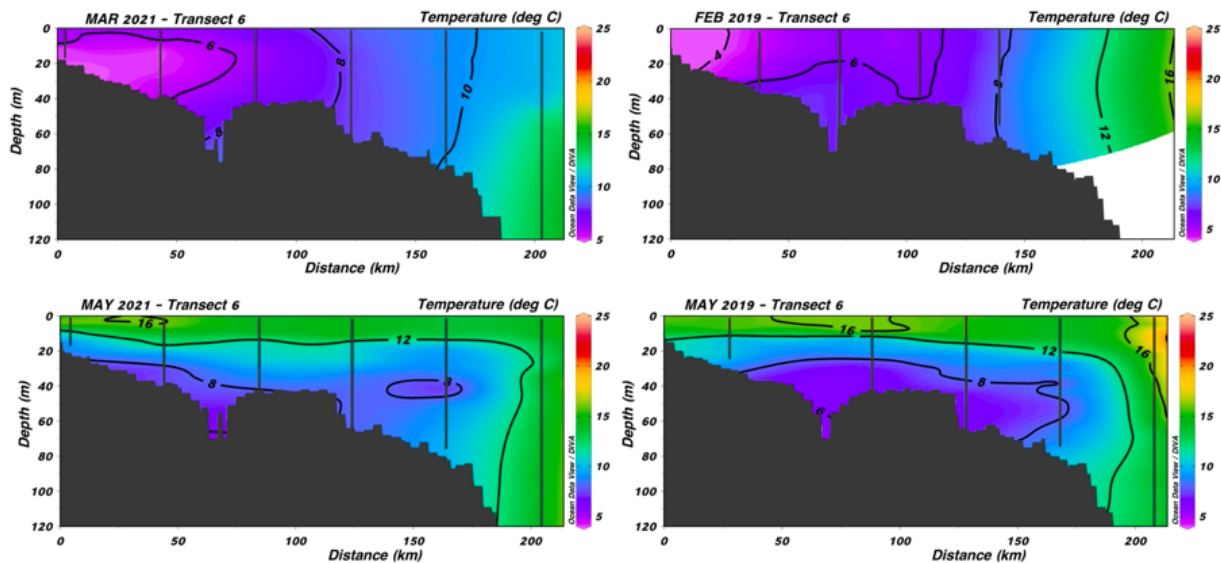


Figure 3. Temperature contours of CTD casts taken on transect 6 to illustrate seasonal and interannual variability in the Mid-Atlantic cold pool, which is defined as bottom water $<10^{\circ}\text{C}$ (purple colors). Transect numbers are labeled in Figure 1 for reference.

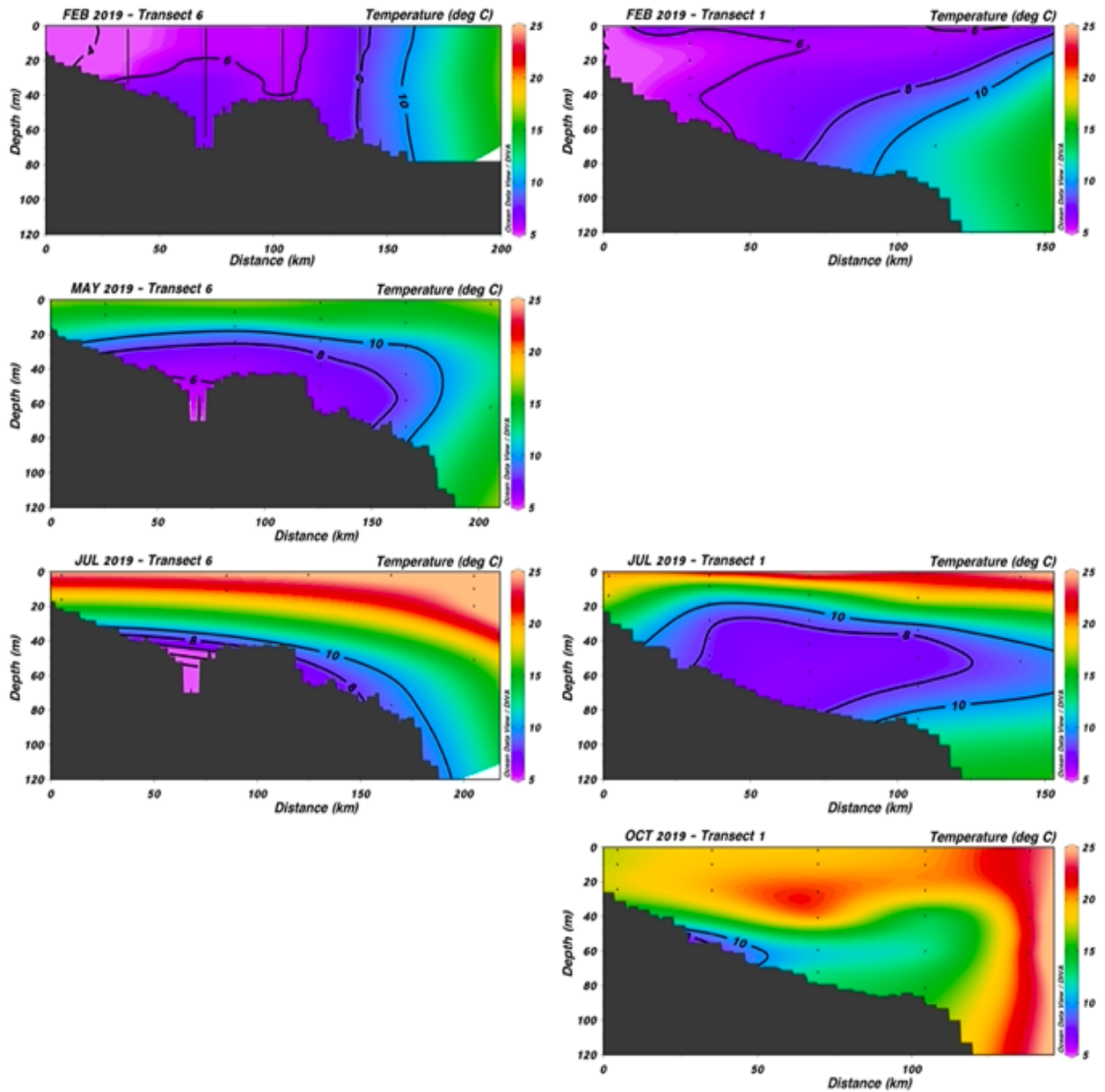


Figure 4. Temperature at transect 1 (right) and transect 6 (left) on the four 2019 cruises. Blank spaces indicate that transect was not sampled. The Mid-Atlantic cold pool is defined here as bottom water <10°C (purple colors). Transect numbers are labeled in Figure 1 for reference.

2.2: Carbonate Chemistry

During this period, we analyzed a total of 656 samples for dissolved inorganic carbon (DIC) and total alkalinity (TA) from the 2019 and 2020 cruises (Table 3). Samples from July 2018 were analyzed for TA and DIC from the NOAA Milford lab using different methods. These data were then used to calculate other carbonate chemistry variables that are important to assessing ecosystem health such as aragonite saturation state and pH throughout the water column.

Table 3. Total number of samples collected and analyzed to date. Cruises denoted with * were analyzed at the NOAA lab in Milford, CT.

Cruise	# samples collected	# samples analyzed for DIC/TA	# samples collected for pH	# samples QA/QC
July 2018*	213	213	N/A	213
February 2019	128	128	N/A	128
May 2019	77	77	N/A	77
July 2019	136	136	N/A	136
October 2019	54	54	N/A	54
February 2020	132	66	66	66
June 2020	62	0	31	0
October 2020	420	195	210	195
March 2021	136	0	12	0
May 2021	246	0	25	0
Total	1604	869	344	869

Using the surface $p\text{CO}_2$ data collected since the beginning of this project, we summarized the spatiotemporal variation of surface $p\text{CO}_2$ in the New York Bight and the Long Island Sound (Figure 5). Surface $p\text{CO}_2$ is a direct measure of air-water gas exchange and the ability of seawater to absorb CO_2 from or release CO_2 to the atmosphere. Seawater is absorbing CO_2 from the atmosphere when the seawater $p\text{CO}_2$ is smaller than the atmospheric $p\text{CO}_2$ which results in

ocean acidification. The atmospheric $p\text{CO}_2$ level is $\sim 400 \mu\text{atm}$ in the study area so the cold colors indicate the ocean is absorbing CO_2 from the atmosphere (Figure 5).

In winter and spring, the New York Bight and the Long Island Sound were generally absorbing CO_2 from the atmosphere, showing $< 400 \mu\text{atm}$ seawater $p\text{CO}_2$ values. The late spring is a transitional period indicated by $> 400 \mu\text{atm}$ surface $p\text{CO}_2$ in some offshore waters and the Long Island Sound. In summer, overall the study area showed to be a CO_2 source with respect to the atmosphere but with complex distribution patterns. Generally, seawater in the Long Island Sound and inshore waters had higher $p\text{CO}_2$ than the offshore water. In fall, seawater $p\text{CO}_2$ increased in the Long Island Sound and inshore waters while decreased in offshore waters, particularly seawater $p\text{CO}_2$ in most offshore waters were $< 400 \mu\text{atm}$. These observations showed clear seasonal variation with complex distribution patterns over time as well as varying magnitude of seawater $p\text{CO}_2$ even if sampled the same month (e.g. May 2019 versus May 2021). It highlights the importance of continuous field monitoring over a wide area to understand how much CO_2 the study area could absorb to lead to ocean acidification and how much temperature, salinity and biological production modify or enhance this process.

Spatial heterogeneity of seawater $p\text{CO}_2$ is significant in the New York Bight and the Long Island Sound. Four featured regions include the Long Island Sound and inshore water, Hudson River Plume area, offshore water on the shelf, and offshore water on the slope. Seawater in the Long Island Sound and inshore water has the largest variation in $p\text{CO}_2$, showing large amounts of CO_2 absorption in cold seasons and CO_2 release in hot seasons. The high $p\text{CO}_2$ in these areas is a result from direct human activity inputs, limited water exchange, higher temperature, and biogeochemical processes releasing CO_2 . The Hudson River Plume area showed very low surface $p\text{CO}_2$ as shown in May 2021, July 2019, and October 2020, in the northwestern region of the New York Bight. As river water typically carries very high $p\text{CO}_2$ and high nutrients, the low $p\text{CO}_2$ in the plume was usually accompanied with high $p\text{CO}_2$ in the water upstream, indicating that the low $p\text{CO}_2$ in the plume is likely a result of high biological productivity supported by the nutrient input. However, this pattern was not observed in July 2018. We are analyzing this data to understand the timing and controlling factors of the low $p\text{CO}_2$ in the Hudson River plume area. The offshore water showed spatial differences in $p\text{CO}_2$ between the eastern and western areas on the shelf while the differences are smaller on the slope. The field observations suggest that the stress of ocean acidification on the health of the ecosystem is likely different in various regions, so maintaining good spatiotemporal monitoring of carbonate chemistry is important.

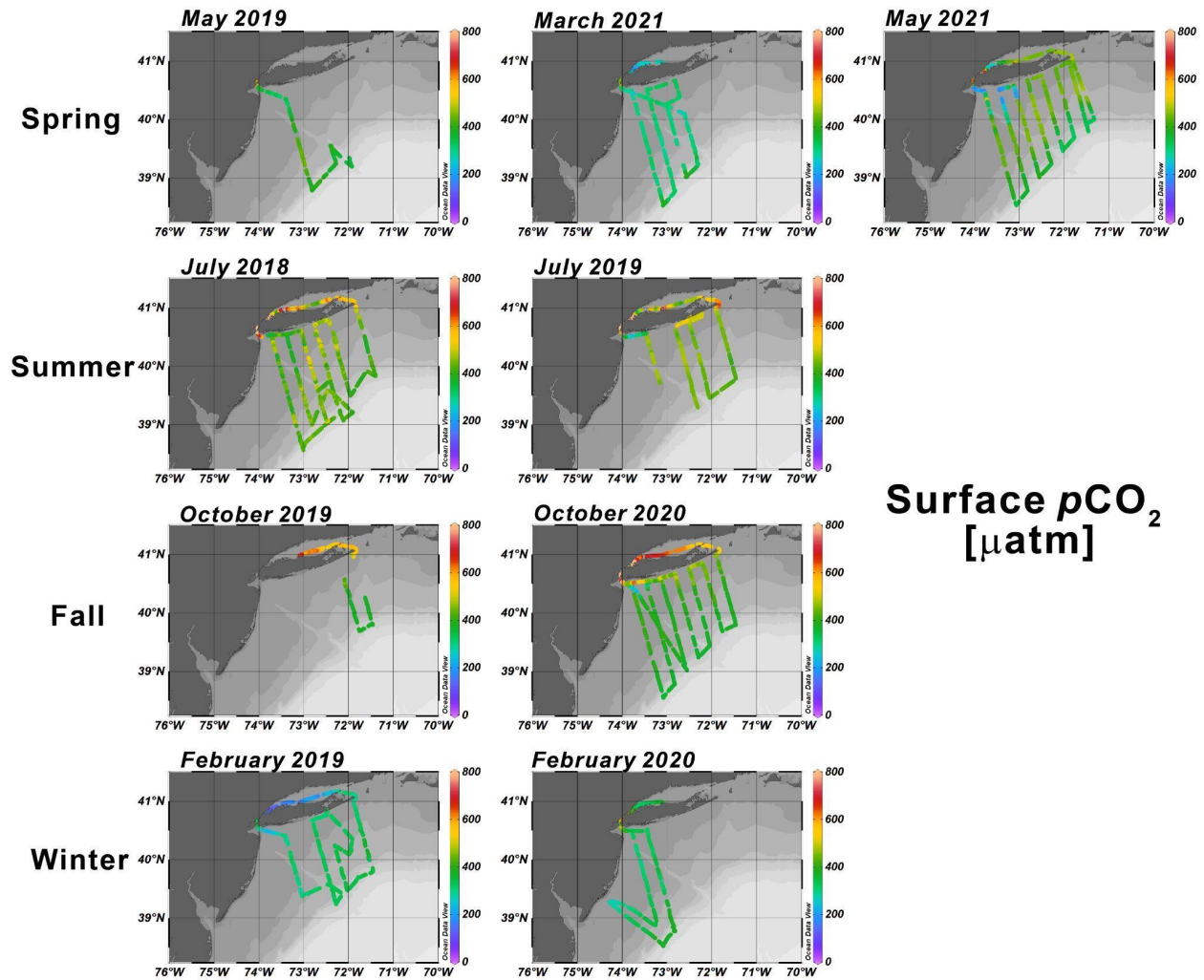


Figure 5. Seasonal maps of surface water $p\text{CO}_2$, an indicator of the ability of the ocean to absorb CO_2 from or release CO_2 to the atmosphere. Atmospheric $p\text{CO}_2$ level is $\sim 400 \mu\text{atm}$, Warm colors indicate the ocean is degassing CO_2 to the atmosphere.

It is critical to characterize the relationship between Total Alkalinity (TA) and salinity (Figure 6) so that salinity can be used as a proxy for TA when pH measurements are taken in the absence of other carbonate chemistry species (TA, DIC, or $p\text{CO}_2$). This approach will be taken now that the new instrument on the glider measures salinity and pH from which the other carbonate parameters must be calculated to characterize ocean acidification and carbonate saturation states (aragonite). This year, we have set up and optimized a new instrument to measure TA and analyzed samples collected from many NYOS cruises (Table 3). Given TA is a semi-conservative parameter in ocean mixing, with TA usually varying in the freshwater endmember, the seasonal or interannual variation in the relationship between TA and salinity is usually small in the oceanic water. Our analyzed data showed a very high quality, consistent relationship of TA and salinity in offshore waters (Figure 6). In addition, our data indicates that two endmember mixing schemes, including inshore water and offshore water, dominated our study area. Slight seasonal variation in TA in the freshwater endmember was also reflected by our high-quality data. It highlights the importance of collecting discrete water samples with large spatial coverage and in different seasons to fully understand the health of the ecosystem over time. In general, inshore waters have more variability because of more variable dynamics and stronger biogeochemical processes.

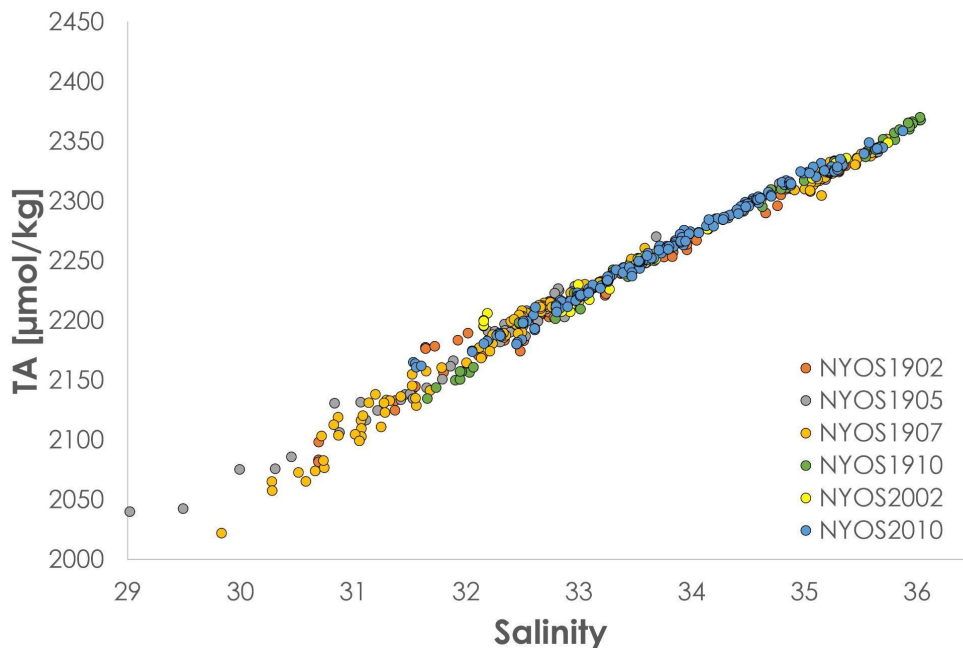


Figure 6. Relationship of total alkalinity (TA) and salinity for discrete samples collected in the six NYOS offshore cruises.

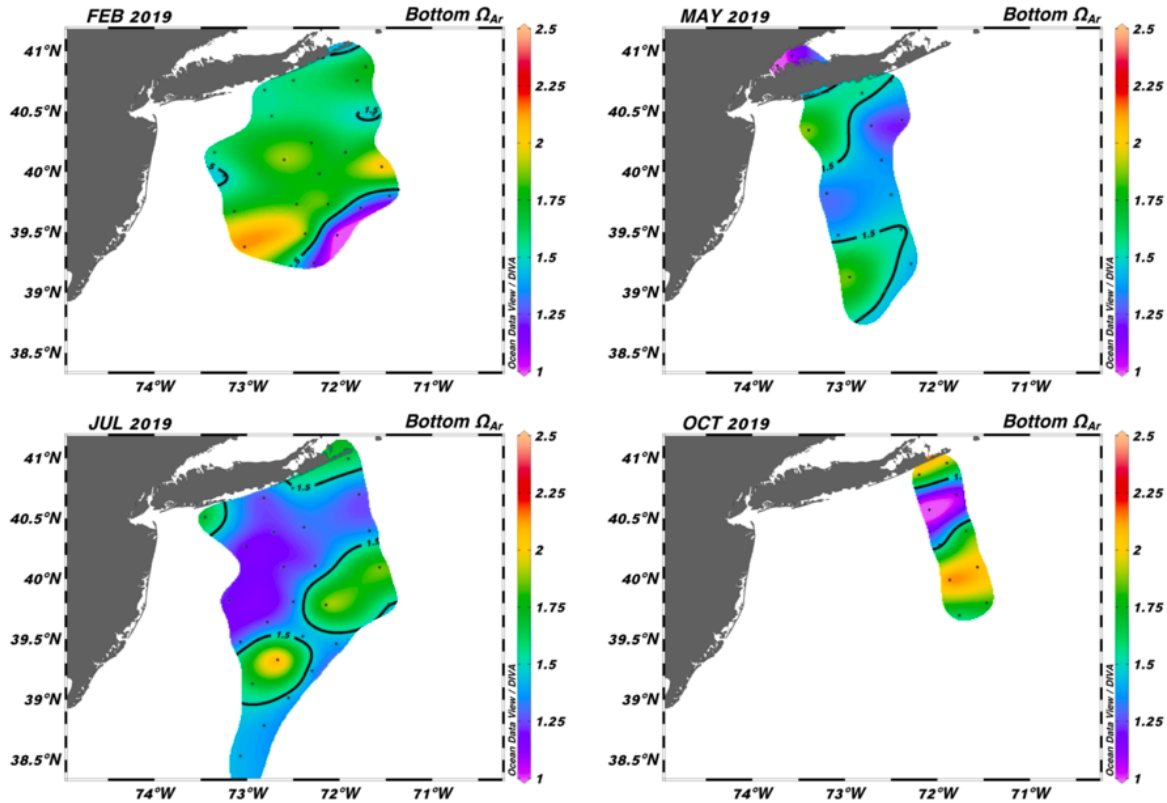


Figure 7. Seasonal bottom aragonite saturation state from 2019 cruises. The contoured areas indicate regions where the saturation state is under 1.5.

With the analysis of all water samples collected on cruises completed in 2019, we were able to use DIC and TA values to calculate aragonite saturation state (Ω_a) and pH, which are the most relevant measures for marine organisms (Figure 7). Understanding Ω_a is critical as many shell-forming organisms utilize aragonite to build and maintain their shells. In order to do this successfully, they require water that is supersaturated. The higher the saturation state of the water, the more calcium carbonate is available in the water to be used for shell formation. Waters with $\Omega_a > 1$ are considered well saturated and suitable for shell formation, while those $\Omega_a < 1$ are stressful for most shell-forming organisms. However, the saturation state that limits growth and survival is species specific so conditions may be stressful as they approach $\Omega_a = 1$. Generally, waters $\Omega_a \leq 1$ are rare in our sampling, but there are consistently large regions approaching this value. For instance, in the top left panel of Figure 6 there are saturation states for February 2019 where a small area of bottom water approach $\Omega_a = 1$ (pink colors) are observed near the deeper waters of the shelf break. Similarly, in July 2019 and October 2019, there are areas in the mid shelf region with water with saturation states near 1. Figure 8 shows the cross section for each transect of the October 2019 cruise, with the area where saturation states are under 1.5 indicated with a contour line. We can see there is a larger area of water near 1.5 on transect 2 compared to transect 1.

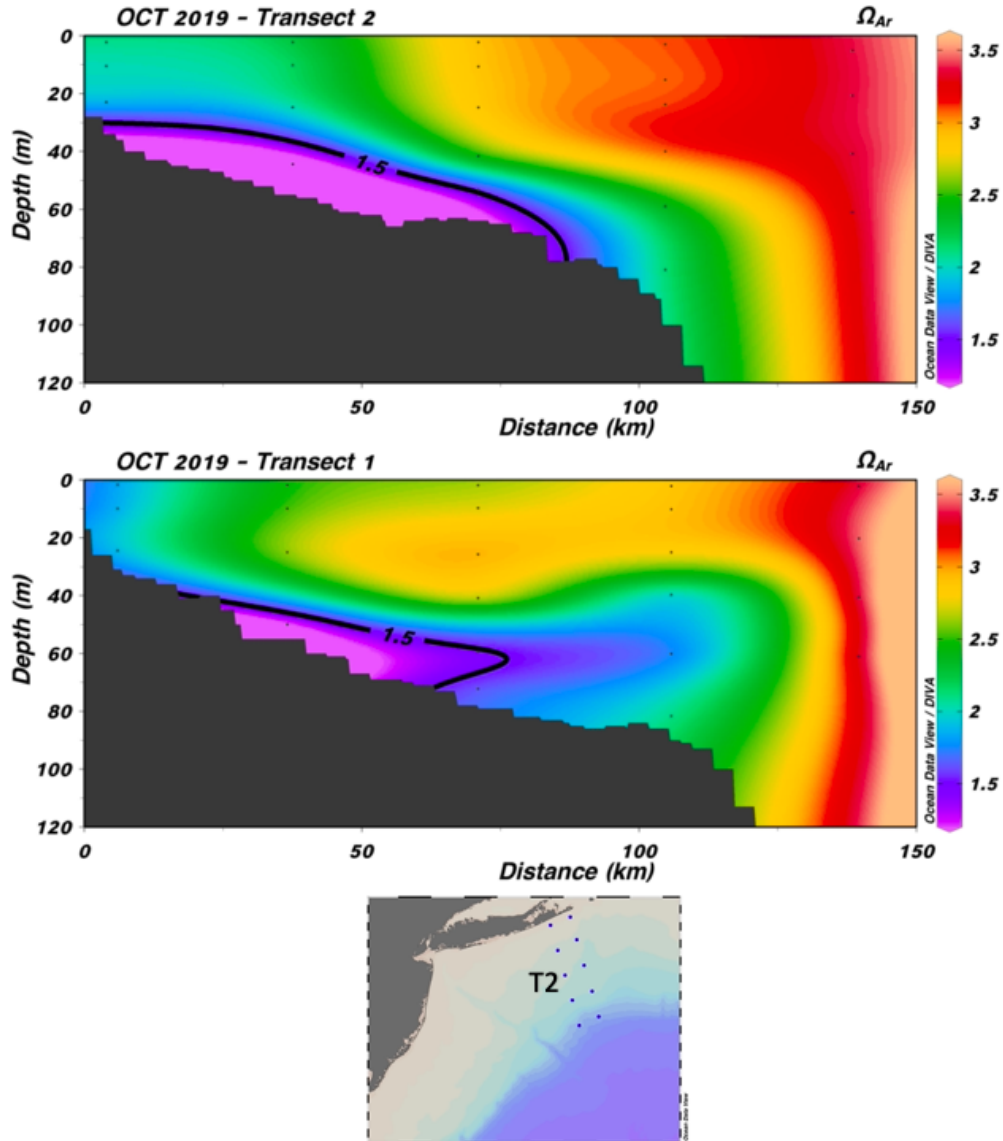


Figure 8. Aragonite saturation state throughout the water column at each transect from NYOS1910. Transect 2 (T2) can be seen on the left side of the map and transect 1 is on the right. The area under the contours represents areas where the saturation is less than 1.5. Transect numbers are labeled in Figure 1 for reference.

Similarly, Figure 9 shows the cross section of aragonite saturation state for each transect on the July 2019 cruise. It is important to note that while there is an area of $\Omega_a \leq 1.5$ at each transect, the exact location and size of the area differs at each transect. In comparing saturation states for transect 1 from Figures 7 and 8, the areas of saturation under 1.5 are quite different in size. Compared to the temperature profiles in Figure 4, the fall is potentially an environmental bottleneck for many shellfish species where aragonite saturation states are at their lowest, but bottom temperature is highest. The combined effect of warm temperatures and low aragonite likely induces higher mortality. From these measurements, we are developing several indicators of carbonate chemistry detailed in the 2021 Indicator report. However, it might be valuable to develop an indicator that considers both temperature and aragonite.

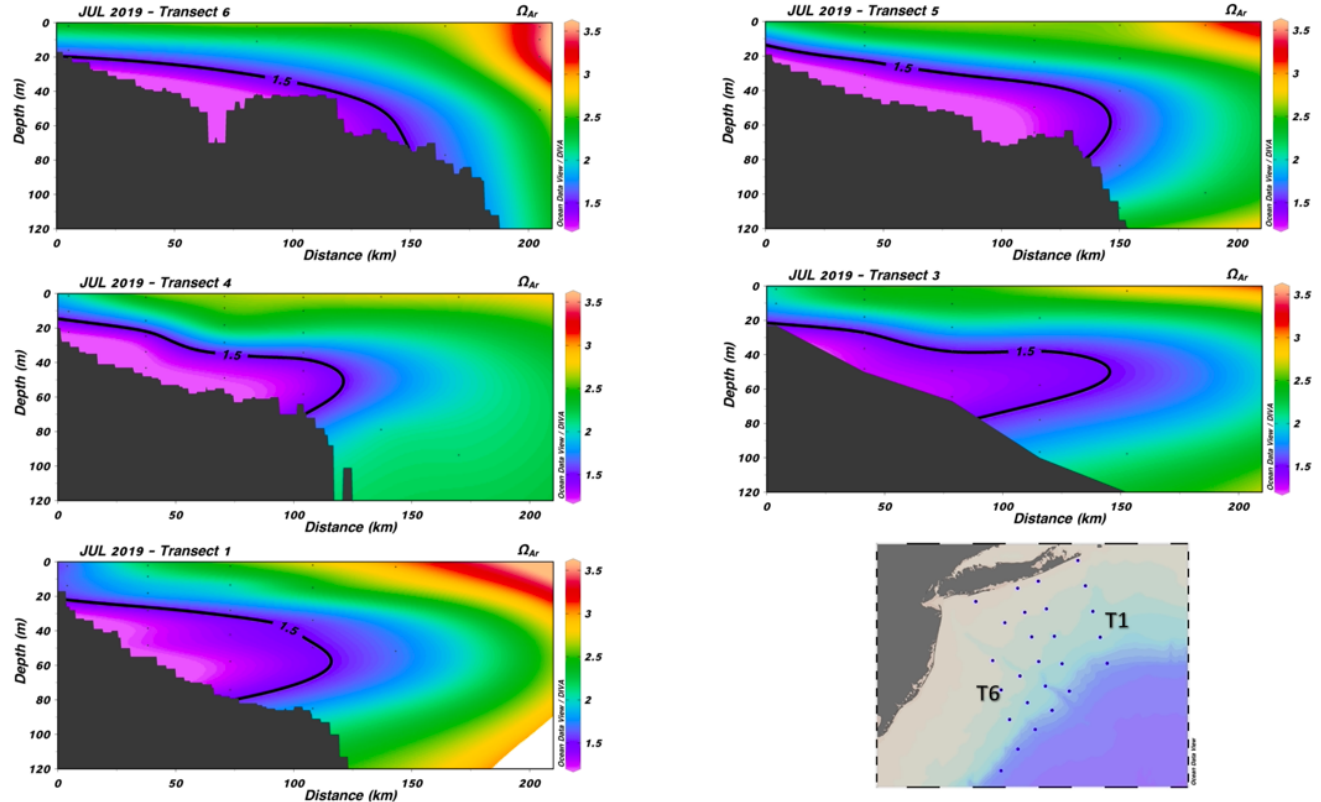


Figure 9. Aragonite saturation state throughout the water column at each transect from NYOS1907. Transect 6 can be seen in the bottom left panel and is indicated by the line of dots next to T6. Transect numbers decrease going east to transect 1 (T1). Transect numbers are labeled in Figure 1 for reference.

2.3: Glider Operations

Calendar year 2021, despite a late start and COVID-19, saw for the first time during our NYB monitoring program a complete seasonal deployment of the glider covering winter, spring, summer, and fall. As a result, by the end of 2021 we have conducted a total of six deployments for a total of 157 days and 4200 kilometers of planned track line, producing on the order of 6000 profiles of temperature, salinity, dissolved oxygen, chlorophyll, and turbidity in the New York Bight (Figure 10). This includes some 4000 profiles of pH since February 2021.

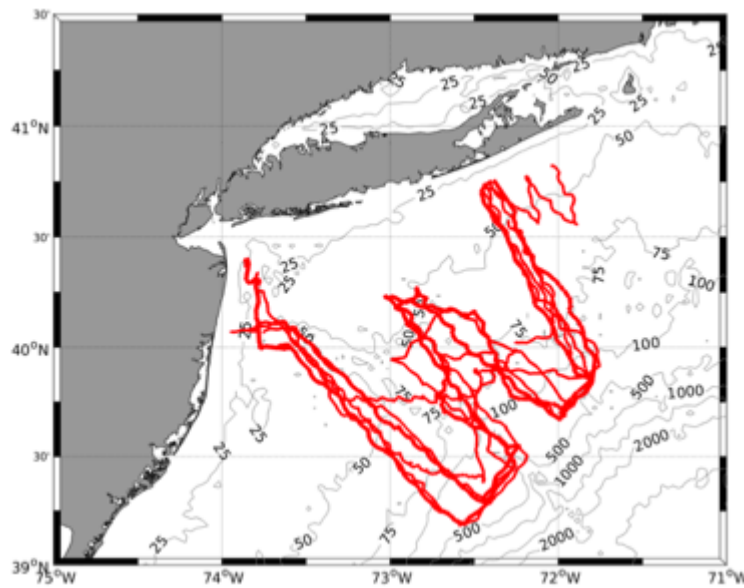


Figure 10. SBU01 glider track lines for all six deployments in the New York Bight.

The latest glider deployment, SBU01_06, took place from November 2 to 20, 2021 for 18 days and covered 522 km. While the deployment was shortened by poor weather for the launch, it was still able to cover the two main east and west transects out to the shelf edge. The intent was to catch the initial collapse of the cold pool, but the launch delay meant that most of the summertime stratification had disappeared while bottom temperatures over the shelf increased from their summer minimums of $\sim 8^{\circ}\text{C}$ to $\sim 16^{\circ}\text{C}$ by mid-November (Figure 11). The shelf waters remained stratified, although it was spread throughout the water column with the highest stratification levels, due to low salinity, in the nearshore waters from Long Island Sound and the Hudson River plume. Offshore, the shelf break front bottomed out around the 60m isobath and was characterized by higher chlorophyll and higher pH levels (Figure 12). Winds during the

deployment were relatively modest so the high turbidity levels along the bottom suggest significant internal wave activity and possible breaking.

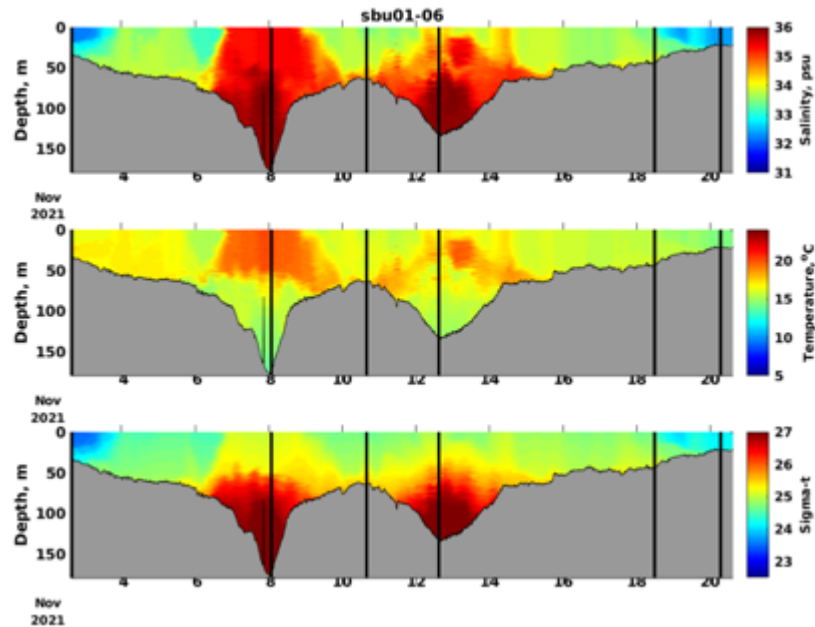


Figure 11. Along-track salinity, temperature, and density plots from the fall 2021 deployment, SBU01_06.

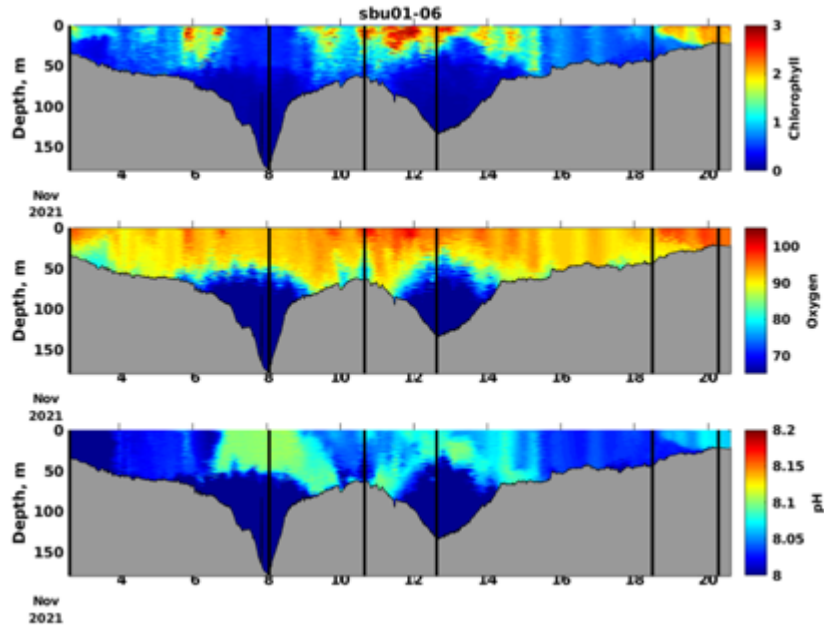


Figure 12. Along-track chlorophyll, dissolve oxygen saturation (%), and pH plots from the fall 2021 deployment, SBU01_06.

Of our six glider deployments, two took place during the time of the summer temperature maximum, one during the coldest part of the winter, one in the spring, and two at various stages during the fall cooling. The range of water properties experienced in the New York Bight, at least in temperature and salinity, is large as shown by the superimposed T/S diagrams in Figure 13. This shows that maximal summer near surface temperatures are more than 25°C over a large range of salinities, minimum temperatures in the cold pool are around 6°C with salinities between 32.5 and 33 psu and slope waters in the outer shelf break front are over 36 psu. Deep slope waters between 150 and 180m depth are around 35.5 psu tending toward the historical values at 1000m of 5°C and ~34.95 psu. Minimum cold pool temperatures fall within a narrow range, but bottom temperatures over the shelf experience a wider range from ~4.5°C in winter to 12 to 15°C during the fall overturning when surface and bottom water mix. Note that the density of the bottom waters remains remarkably constant at ~25.8 sigma-t units throughout the year.

In December 2021, the glider was sent back to Webb Research for sensor calibration and an overall functional checkup. This process takes about three months and has necessitated skipping the winter deployment. The next planned deployment starts in April with the spring cruise. The manufacturer recommends that the gliders are returned for service at least on a bi-annual basis. To deal with this lapse in coverage, we are in the process of ordering a second glider of the same

type so that we can maintain the desired four seasonal cruises a year while being able to send the glider back for calibration. We anticipate that the second glider will be delivered sometime in May or June. The new glider will have the usual suite of sensors with the addition of a DMON3 from Mark Baumgartner's group at WHOI, which can record a wide range of whale calls. In addition to the DMON3 for the new glider, we are teaming with Mike Frisk's group to mount a Vemco receiver on either of the gliders to monitor the local presence of tagged fish as the glider proceeds across and along the shelf.

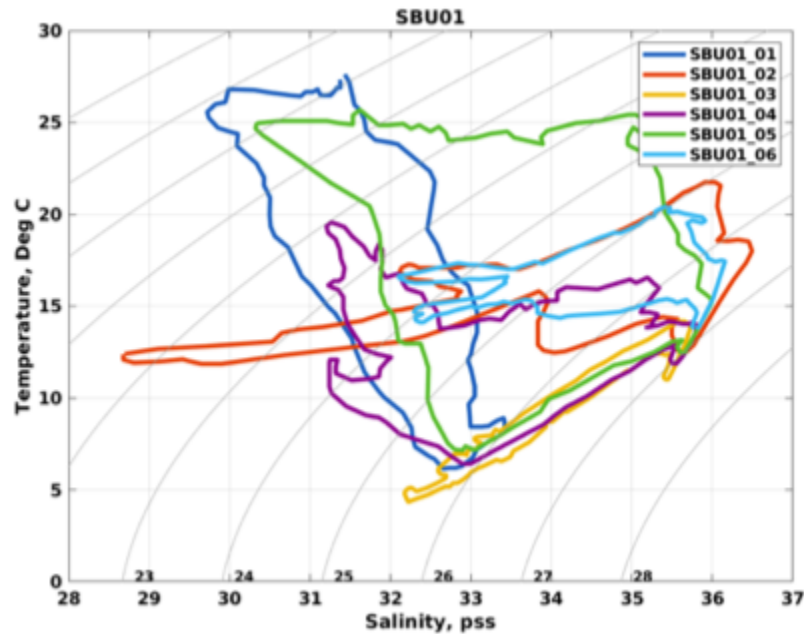


Figure 13. Superposition of the temperature/salinity diagrams from all six deployments showing the range of properties experienced by the waters of the New York Bight. The seasonal deployments covered winter (SBU01_3), spring (SBU01_4), summer (SBU01_1, SBU01_5), and fall (SBU01_2, SBU01_6).

Objective 3: Characterize lower trophic level productivity

Two vertical zooplankton net tows, from 25 m depth to the surface, were conducted at all hydrographic stations during the 2021 offshore surveys, for a total of 126 net tows across 63 station visits. A 60 cm diameter, 333 μm mesh ring net was used for all zooplankton tows. The first set of identical net tows at each station were conducted to collect all zooplankton, and the second was to collect additional data for the new protocol addressing ichthyoplankton identification and distribution. Biovolume was measured for all collected samples. The first tow at each station was preserved in 10% formalin and 90% seawater for later identification, counts, measurements, and photos (Figure 14). The second tows, focused on fish eggs and larvae, were preserved in ethanol for genetic barcoding.



Figure 14. Common zooplankton collected in vertical net tows during the NY Offshore Indicators cruises. Identifications from left to right are: red cyclopoid *Oncaea* sp., echinoderm larvae, copepod *Centropages bradyii*, pteropod *Hyalocylis striata*, and harpacticoid *Miracia efferata*. Black lines on the rulers behind the animals in the images mark 1 mm measurements.

Zooplankton sample processing (identification and enumeration) takes several hours per sample at the stereo microscope. Stereoscope processing was the initial method used prior to obtaining the new ZooScan equipment. Thus, we present results in this report for the 2019 and 2020 cruises as the 2021 samples are still being processed. Mapping distributions of zooplankton abundance can help parse out spatial and seasonal patterns of presence and abundance across multiple species of interest. One of the most abundant zooplankton taxa in the New York Bight is cladocera. This taxa shows seasonal changes, with lowest abundance in the winter, peak abundance in the summer, and decreasing abundance in the fall of 2020 (Figure 15).

Ecologically important and abundant copepod species can also be compared spatially. Higher abundances of *Centropages typicus* are caught during inshore net tows at shallower depths, while *Calanus finmarchicus* are caught at higher abundances during offshore net tows in deeper waters during the May 2019 cruise (Figure 16).

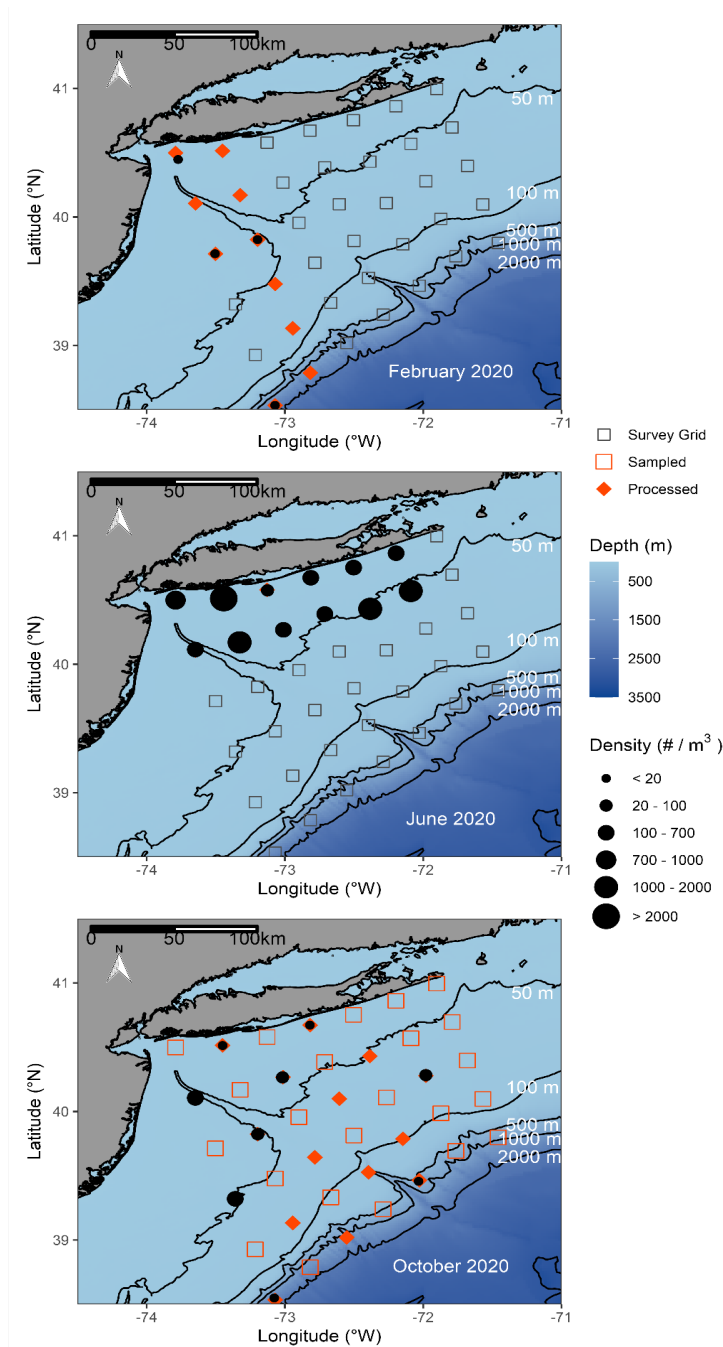


Figure 15. Spatial distributions of all cladoceran species for each of the 2020 cruises, in February, June, and October 2020. The full survey grid includes 39 stations (open gray squares), but due to cruise conditions, net tow sampling was only conducted at some stations (open orange squares), and due to long processing times, a subsample of collected samples was processed (filled orange diamonds). The black circles show the relative densities of cladocerans at sites where they were present. Cladocerans were most abundant in June. However, only samples from inshore stations were collected and processed.

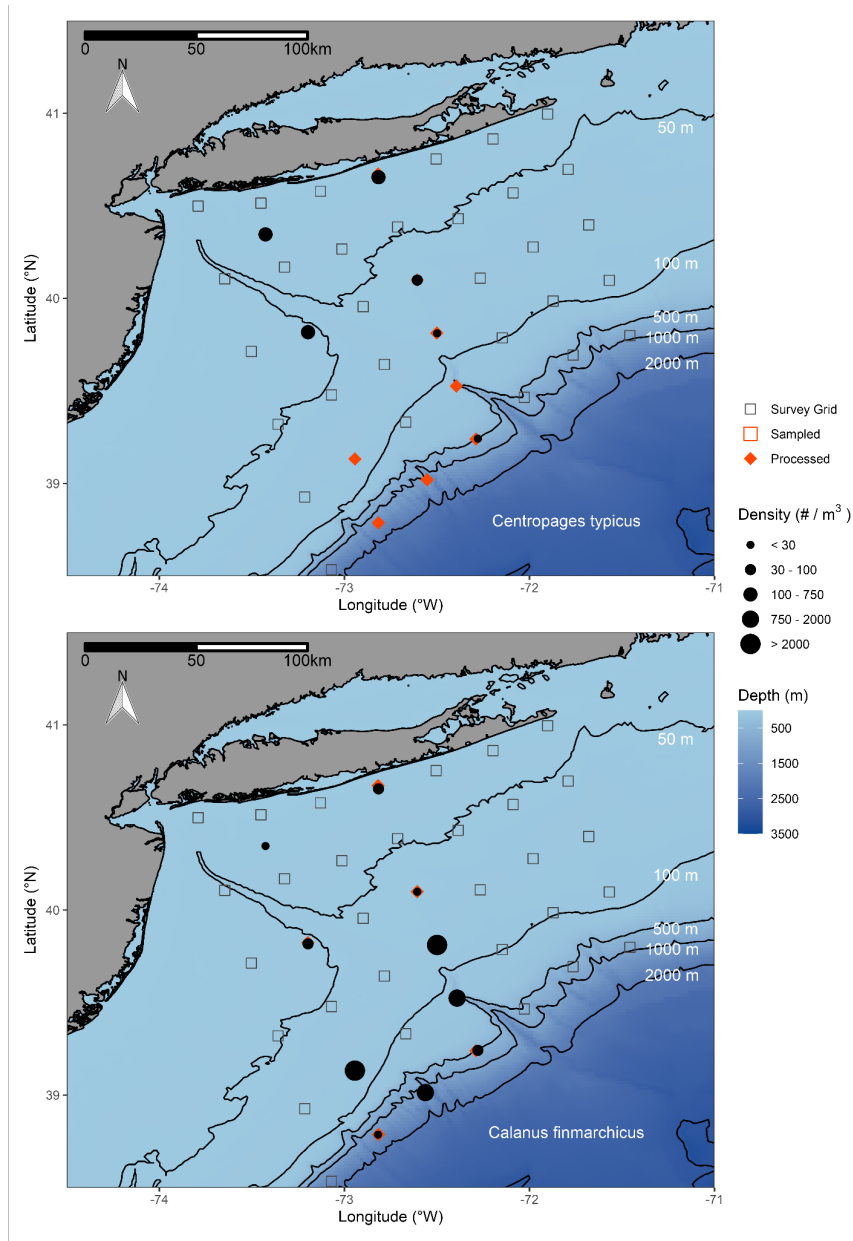


Figure 16. Spatial distributions of two of the most abundant copepod species from the May 2019 cruise, *Centropages typicus* and *Calanus finmarchicus*. The full survey grid includes 39 stations (open gray squares), but due to cruise conditions, net tow sampling was only conducted and processed for some stations (filled orange diamonds). The black circles show the relative densities of copepod species at sites where they were present. *Centropages typicus* densities were higher at inshore stations compared to *Calanus finmarchicus*, which dominated offshore stations.

Post-cruise sample processing (enumeration and identification) in the lab is completed for all samples through the October 2020 cruise (NYOS2010). The NYOS ZooScan learning set (for automatic categorization of taxa) is built and completed, and the Warren Lab is now finalizing student training and protocols for using the ZooScan system to streamline the zooplankton processing procedure. Capturing images of animals with use of the ZooScan (Figure 17) eases the identification process.

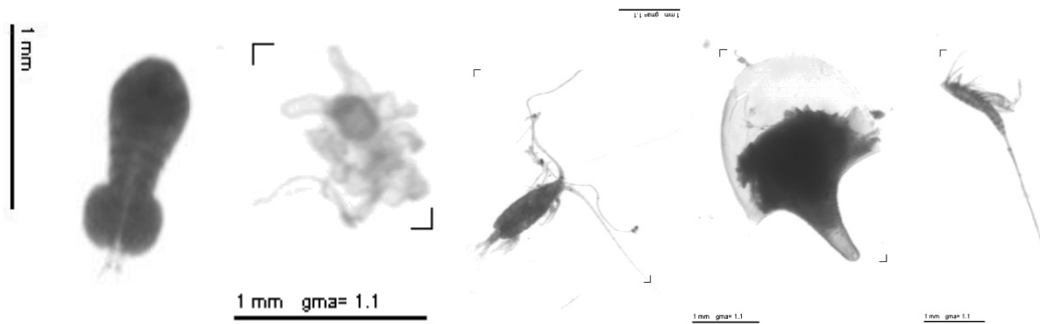


Figure 17. Images produced from the ZooScan system from multiple 2020 cruises. Animals from left to right are: cyclopid *Oncaea* sp., echinoderm larvae, copepod *Centropages bradyii*, pteropod from Subfamily Cavaliniinae, and harpacticoid *Microsetella norvegica*. Scale bars in each image represent 1 mm.

We have continued to examine lower trophic level prey quality through images of individual copepods. Prey quality measurements have been focused on the calanoid copepod, *Calanus finmarchicus*. Images have been annotated using ImageJ software to measure the length and area of animal prosome and internal lipid (oil) sac. From these measurements, the lipid ratio (lipid sac area divided by prosome area) is calculated. Preliminary data show variability in lipid ratio across stations within a cruise (Figure 18). These preliminary findings between lipid ratio and net tow will be further explored to assess statistical relationships as well as patterns associated with environmental variables. The data also suggest some seasonal variation in the prosome length of the copepods (Figure 19).

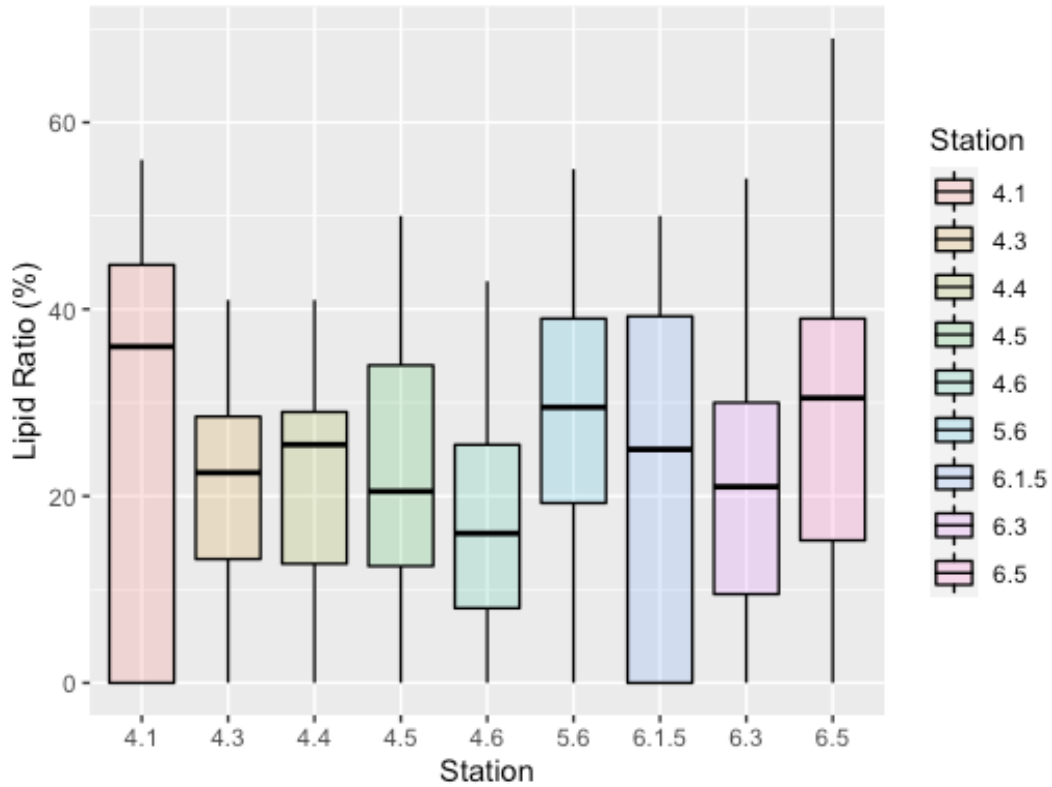


Figure 18. Lipid ratios varied between 0 and 69% for 30 copepods measured at each station during the May 2019 cruise. The highest variability in *Calanus finmarchicus* lipid ratio can be seen at stations 4.1 and 6.1.5. The lipid ratio was lower at station 4.6 compared to 5.6 and 6.5. Transect numbers are labeled in Figure 1 for spatial reference.

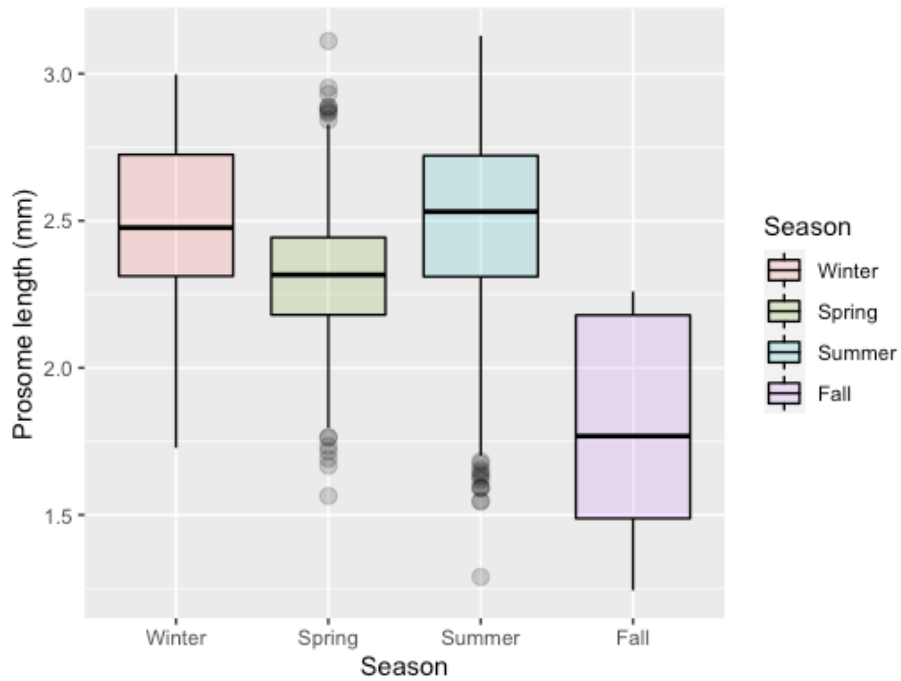


Figure 19. Prosome lengths of Calanus finmarchicus were smallest (but most variable) in the fall compared to all other seasons. Four winter, nine spring, seven summer, and two fall stations were included in this data set and each station had 30 measured copepods representing it.

Objective 4: Quantify abundance and distribution of pelagic fishes and squid in the New York Bight.

Multiple-frequency (38, 70, 120, and 200 kHz) scientific echosounders are used to record the backscatter from pelagic fish and squid from a few meters below the surface to the seafloor continuously during each survey (Figure 20). Acoustic surveys are widely used throughout the world to assess fish stocks and in conjunction with net trawl ground-truthing this method can provide quantitative measurements of distributions of pelagic fish and squid abundance. Acoustic backscatter measurements are processed to remove noise and scattering from non-biological sources (mostly bubbles near the surface produced by wind and waves). The backscatter at each individual frequency is then integrated both horizontally and vertically to produce estimates of the nautical area scattering coefficient (NASC, m^2/nmi^2) which is proportional in many cases to organism biomass. Fish with swimbladders scatter sound differently than swimbladderless fish or crustacean zooplankton.

These differences can be exploited by combining information from two or more frequencies to identify and discriminate backscatter caused by swimbladdered fish or other scatterers. These processed data also allow for seasonal and geographic comparisons across the different cruises (Figures 21-22). It's important to remember that the y-axes at each frequency within the figures are not the same because NASC values are not directly comparable across frequencies.

Although there may sometimes be qualitative relationships between different frequencies (Figure 22), plotting NASC across seasons may help characterize years with relatively high NASC across all frequencies, and therefore indicating months, seasons, or years with generally higher biomass estimates. For example, backscatter at 200 kHz tended to be higher during the spring and winter months, backscatter at 38 kHz tended to be higher the summer and fall months, and backscatter at both 70 and 120 kHz were pretty variable year-to-year across seasons (Figure 22).

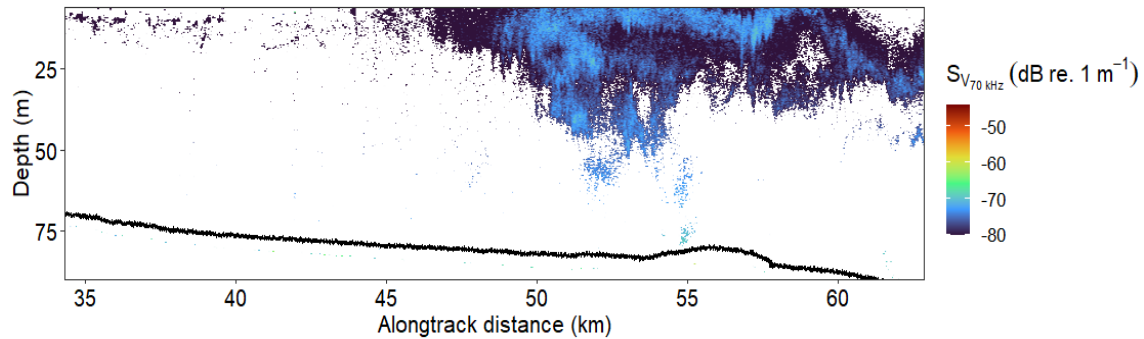


Figure 20. An echogram at 70 kHz from the May 2021 (NYOS2105) cruise showed the presence of weakly scattering aggregations that likely represent small fish, squid, and crustacean zooplankton. These data were collected from Transect 01 at depths less than 100 m. The black line represents the seafloor. Point color represents S_v (dB re. 1 m^{-1}), which is the integrated, volumetric backscatter for that part of the water column.

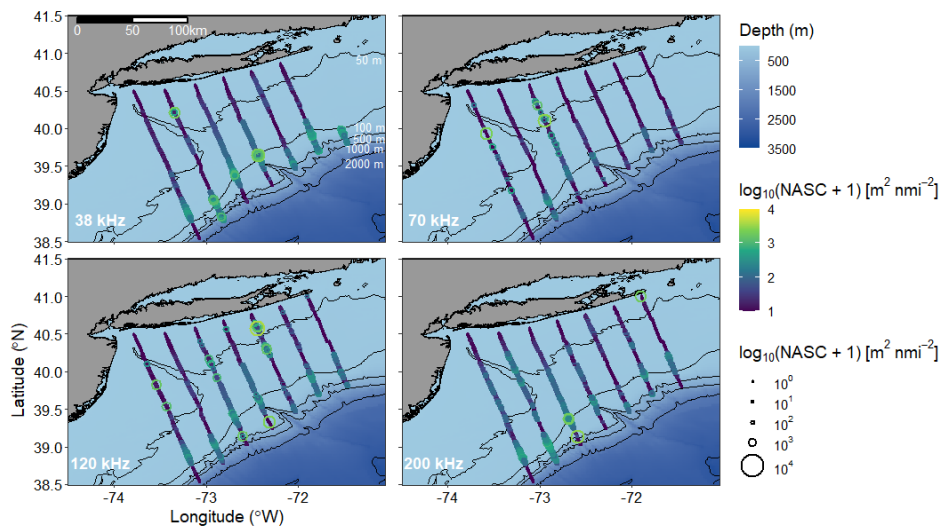


Figure 21. Fishery acoustic surveys produce spatial maps of NASC ($\text{m}^2 \text{ nmi}^{-2}$). Here each panel represents NASC for a different frequency measured during the May 2021 cruise. The color and size of each circle are scaled to how much backscatter occurred at that location. For many species of interest, NASC will be proportional to animal biomass with lower frequencies (38 and 70 kHz, top panels) measuring swimbladdered fish and squid, while higher frequencies (120 and 200 kHz, bottom panels) measuring swimbladderless fish and/or zooplankton. These maps can be used to identify areas where pelagic fish and zooplankton regularly occur, which can be useful for marine planning purposes.

Stony Brook University, Stony Brook, NY 11794-5000
 Tel: 631-632-3187; Fax: 631-632-8820

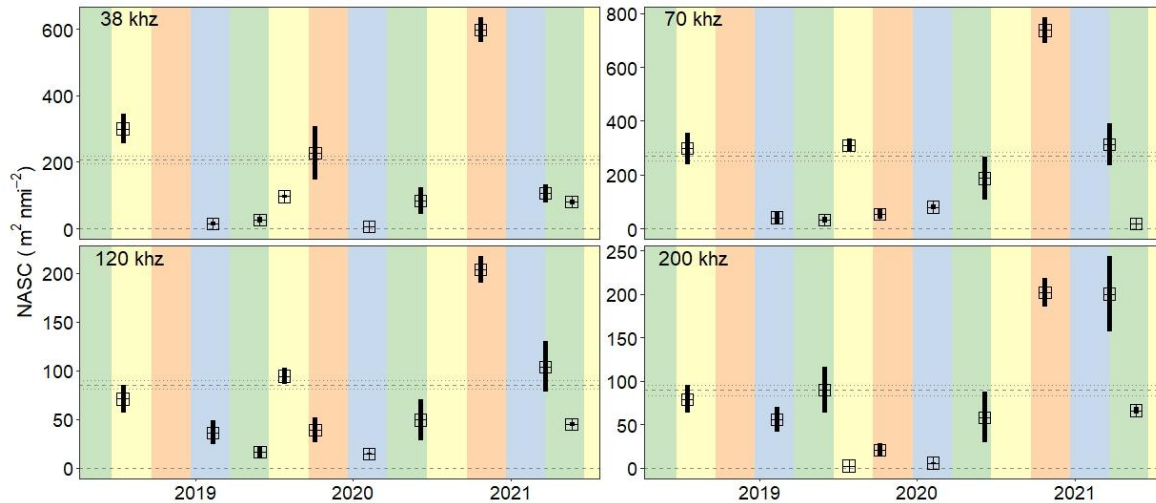


Figure 22. Seasonal trends in NASC ($m^2 nmi^{-2}$) were tested using the stratified means (crossed-boxes) and 95% confidence intervals (lines) at each frequency using an algorithm adapted from Jolly and Hampton (1990). The background colors represent spring (green), summer (yellow), fall (orange), and winter (blue). The horizontal dashed lines represent the stratified mean NASC and 95% confidence intervals for each frequency. Note that the y-axes at each frequency are not the same since NASC values are not directly comparable across frequencies. These summary statistics can be used to view broad seasonal trends in backscatter at each frequency.

Objective 5: Collect opportunistic sighting and behavioral data of cetaceans in the New York Bight

5.1 Seabird and Marine Mammal Line-transect Surveys

Due to the ongoing COVID-19 pandemic, all R/V Seawolf cruises in 2021 were operated with reduced crew and thus it was not possible to send an observer team on these cruises. As a result, no line-transect surveys were conducted in 2021. In previous years, line transect surveys focused on marine mammals. However, we reprioritized the taxonomic focus of these surveys to focus on seabirds and designed a standardized distance sampling survey for seabirds (Buckland et al. 2001), which will be implemented during future surveys. Our survey design closely follows methods as outlined in Gjerdrum, Fifield, and Wilhelm (2012) with a few exceptions: we will collect more detailed and comprehensive distance sampling data, including radial distances and bearings from which perpendicular distances and sighting location can be derived. These surveys will allow us to examine seabird abundance, distribution and broad behavioral classes throughout the New York Bight. We designed a custom data collection template in Mysticetus software and integrated speech recognition functionality using Nuance Dragon NaturallySpeaking software and simple visual basic scripts. This allows observers to collect data hands-free and allows them to auto-populate critical fields with voice command in real-time while using other survey field tools (e.g. binoculars, pelorus). It also allows surveys to operate with full coverage with one less observer than we had used previously during marine mammal surveys as we no longer need a midship observer serving primarily as data entry. We plan to deploy this new survey system in the 2022 winter cruise to initiate standardized data collection on seabird abundance and habitat use in the NYB. Line-transect surveys are conducted concurrently with oceanographic and fisheries acoustics surveys, and ongoing integrative analyses of these interdisciplinary datasets will allow us to better understand drivers of seabird abundance and distribution and trophic interactions between mid and upper trophic levels through the course of this monitoring program (Objective 6).

5.2 UAV surveys of humpback whales and ongoing body volume and body condition analyses

The NYB provides important foraging habitat for humpback whales during summer months, when humpback whales build up energy stores to use when fasting during the breeding season (Lockyer, 1987; Christiansen et al. 2016, Brown et al. 2018). Little is known about foraging behavior and health of humpback whales in the NYB. To address these gaps in knowledge and to provide an indicator of resource availability in the NYB through time, we are quantifying the body size and body condition of humpback whales using UAV measurements (Groskreutz et al. 2019) and assessing humpback whale foraging behavior in the NYB.

In 2021, we continued our photogrammetry study of humpback whales in the NYB using unoccupied aerial vehicles (UAV). In previous years (2018-2020), we collected data on foraging behavior and length of 52 humpback whales observed between 0.37-86.3 km from the south shore of Long Island. We found that juveniles were exclusively found within 10 km of the coastline and foraged independently in this region by surface lunge feeding on dense schools of Atlantic menhaden. Both juvenile and adult whales were observed more than 10km from shore, where cooperative foraging behaviors were observed. The erratic lunge feeding behavior of juvenile humpback whales close to shore, where vessel traffic is dense and fast, suggests that these whales could be at particular risk of vessel strike (Stepanuk et al., 2021).



Figure 23. Example of aerial imagery of humpback whales obtained during the 2021 field season.

In 2021, we conducted 2249 km of opportunistic UAV surveys over 15 field days aboard the R/V Parker operating out of Stony Brook University's Southampton Marine Research Station to assess humpback whale body condition in the NYB. A total of 27 individual humpback whales were observed in 2021 (two individuals were sighted on multiple dates), with sightings occurring on 11 of 15 days (Table 4; Figure 24). Six days of survey effort were conducted in offshore waters (>10km from shore) but no UAV imagery was obtained for humpback whales in offshore waters. While two humpback whales were observed offshore on one survey day (May 21), conditions did not allow the UAV to be safely launched. One humpback whale was observed briefly offshore on August 10 but was not observed again after the initial cue. Thus, all morphometric data in 2021 was collected on individuals seen close to shore (<10km), and all individuals were classified as juveniles based on a length threshold of 12m (Stepanuk et al. 2021). UAV imagery suitable for morphometric measurements such as in Figure 23 was obtained for 17 individuals (measurement protocol described below). No cooperative foraging behaviors were observed in 2021, though 8 sightings had surface lunge events and there was one observation of a single-animal bubble net 3.4 km from shore.

*Table 4. Summary of UAV survey effort (time and distance surveyed), the number of humpback whales (*Megaptera novaeangliae*) observed, and the number of whales for which we were able to obtain body length and body volume measurements, respectively. Offshore effort refers to effort that primarily occurred more than 20 km from shore based on observations of inshore / offshore age-based partitioning of juveniles and adult humpbacks in Stepanuk et al. 2021 * Indicates one individual was resighted (once on both July 20 and August 3, 2021 and once on July 20, 2021 and August 25, 2021).*

Survey Day	Survey Area	Effort Hours	Effort Distance (km)	No. humpback whales sighted	No. humpback whales - body volume
2021-05-21	Offshore	6.2	186.8	2	0
2021-06-02	Offshore	5.5	176.1	0	0
2021-06-24	Inshore	7.7	173.6	1	1
2021-07-20	Inshore	9.6	177.3	3	2
2021-07-24	Offshore	10.0	204.4	1	0
2021-07-27	Offshore	8.7	190.6	0	0
2021-08-03	Inshore	9.1	104.7	4*	3
2021-08-04	Inshore	7.3	76.9	2	1
2021-08-10	Offshore	8.3	244.5	1	0
2021-08-25	Inshore	7.6	108.1	3*	3
2021-08-27	Inshore	6.6	97.4	2	1
2021-08-31	Offshore	7.5	228.0	0	0
2021-09-14	Inshore	6.5	95.2	1	1
2021-10-07	Inshore	5.8	73.3	5	4
2021-10-15	Inshore	8.2	112.0	4	3

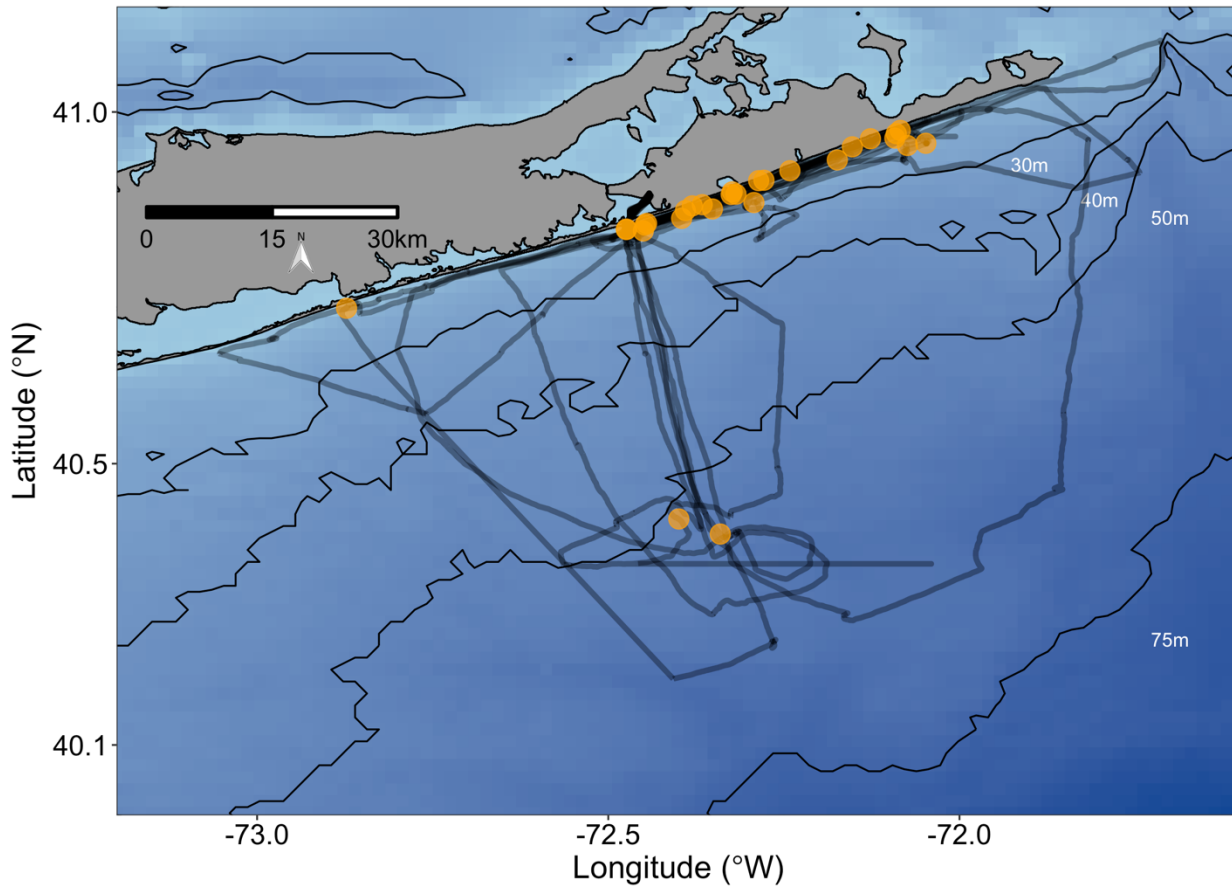


Figure 24. Small-boat UAV survey effort (dark grey) and humpback whale (*Megaptera novaeangliae*) sightings (orange) during the 2021 field season. All humpbacks for which we were able to capture aerial imagery occurred inshore and derived lengths suggest they were juveniles. In contrast to previous years, we only observed two humpback whales in offshore waters, but conditions prevented the crew from tracking these animals long enough to obtain aerial footage. All surveys were conducted from R/V Parker.

Body condition estimates were generated using morphometric measurements of still images obtained from the UAV video for all flights conducted between 2018 and 2021. Images first were scored by two independent analysts for focus, animal body position (e.g. straightness, roll, arch, pitch), and overall width and length measurability, as in Christiansen et al. (2018). A ranking system was used for each category with a score of 1 representing ideal or near ideal attributes (e.g. for straightness, the body axis midline crosses the peduncle closer to the center than to the edges), a score of 2 representing imperfect, but still serviceable attributes, or a score of 3 representing attributes that are too poor quality. Images which scored a 3 in any of the aforementioned image attribute categories or a 3 in the overall width measurability (e.g. body outline not discernable over large areas) were determined unsuitable for body volume measurements and discarded from future analyses. A full description of each image attribute and scoring metrics is available in Supplementary Information Table S1 in Christiansen et al. (2018). A single best image was chosen for each individual. In total, imagery suitable for morphometric measurements (body length and volume) was obtained for 59 whales, including 17 individuals from 2021 (Figure 24). Individual lengths and widths (at 5% intervals) were measured in the MorphoMetriX (Torres and Bierlich, 2020) and were collated with the Collatrix (Bird and Bierlich, 2020).

While many estimates of body condition assess dorsal area of whales visible from UAV images, assessing volume provides a more holistic means of characterizing body condition that is also useful in a range of morphological and biological studies. To facilitate the development of volumetric estimates of humpback whale body condition, we developed 3D models of whales that are integrated with morphometric measurements from UAV surveys to produce body condition estimates of individual whales. We developed 3D models of both adult and juvenile humpback whales in Blender, open-source modeling software (Community, B. O., 2018). Initial models were scaled using 17 width measurements (taken at 5% intervals of total body length, except for the intervals posterior to 85% total length, which are grouped into one region), height-width ratios, and total length (Figure 25). This 3D model represents an improvement of traditional geometric means of estimating cetacean volume (e.g., the truncated cones method), as the model conserves external morphology rather than estimating the body shape based on geometric approximations. We quantified how many, and which, morphometric measurements are required to accurately model humpback whale morphology and volume by assessing the error produced by all possible combinations and numbers of the 18 morphometric measurements (17 widths and total body length) obtained from UAV images (Hirtle et al. in review). Comparisons to previous geometric estimates of cetacean body volume demonstrate that our 3D model is more accurate, particularly when using fewer morphological measurements. Our findings suggest that by conserving the external morphology of cetaceans rather than approximating morphology using geometric shapes, 3D models present a major advantage for estimating body volume and body condition. The ability to accurately estimate body volume with a comparatively small number of measurements will allow a larger sample size in analyses as some measurements often cannot be obtained for an individual whale due to water quality or image characteristics (e.g., dorsal widths obscured by blow, arched body position).

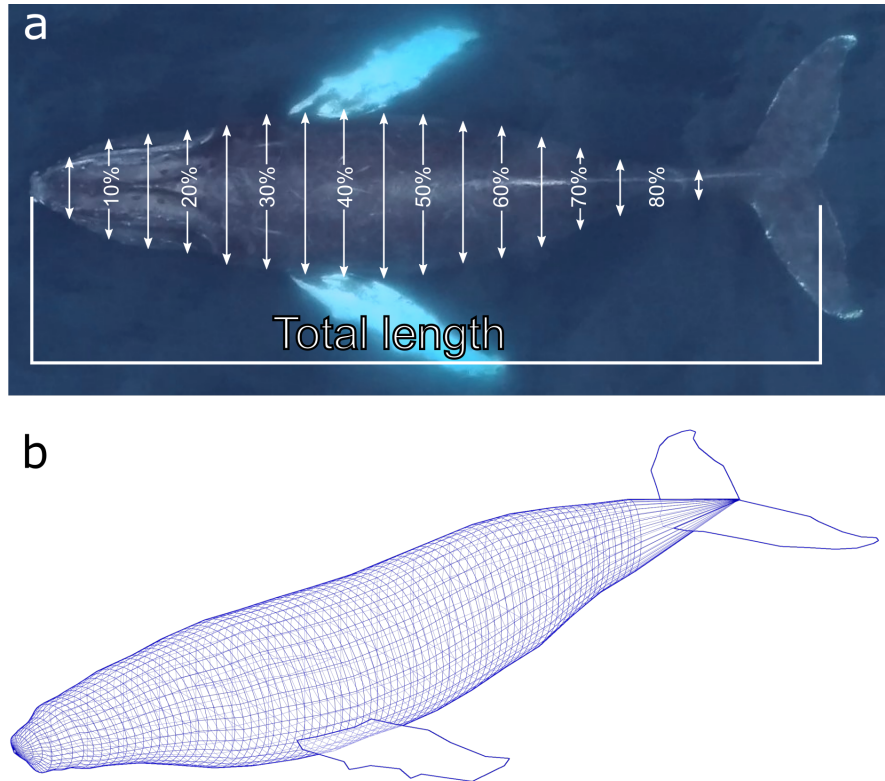


Figure 25. a. Example of a still image captured from UAV aerial image of a humpback whale showing width measurements taken at 5% intervals of body length. b. These measurements are then used as inputs to scale 3D models and obtain volumetric estimates of humpback whales.

Since humpback whale body condition is expected to improve as whales increase their energy reserves over the course of a foraging season, it is necessary to quantify within-year variability in body condition in order to generate a reliable indicator of humpback whale body condition that can be compared across years. Juvenile and adult whales accumulate energy reserves differently (Christiansen et al., 2016) and we therefore assessed patterns in body condition (body volume) of these two age classes separately. Since observations of humpback whales in the NYB are dominated by juveniles, our sample size for juvenile measurements is larger and we focused on juveniles for preliminary modeling and indicator development.

Following exploratory data analyses to assess linearity of model terms, we used a generalized linear model (GLM) to assess how the following variables influenced body volume in humpback whales: day of year (reflecting seasonal accumulation of energy reserves), total length (to

account for differences in body size), and year (reflecting inter-annual variability in the accumulation of energy reserves). The final model, selected using Akaike's Information Criterion (AIC), performed well in explaining variability in humpback whale body volume within and between years (p value = 2.34×10^{-10} , adjusted $R^2 = 0.71$, deviance explained = 49.6%). All years other than 2018 showed significant changes in body volume during the foraging season, likely due to the small sample size and limited temporal coverage in 2018 (all measurements were obtained between July 16 and August 24 in 2018 while measurements obtained during 2019, 2020 and 2021 covered time spans of approximately 5-6 months). Our preliminary results suggest that juvenile humpback whales exhibited substantial variability between years in the accumulation of body reserves. While body volume increased similarly throughout the foraging season in both 2020 and 2021, body volume increased more rapidly through time in 2019. In addition, the overall body volume of juvenile whales was higher in 2020 than in 2021.

Objective 6: Characterize trophic interactions and oceanographic drivers of living marine resources

Several indicators of oceanographic habitat (cold pool extent and duration, location of the 20°C isotherm) have been developed by postdoc Laura Gruenburg that will be used to examine relationships between physical conditions and upper trophic levels. She is currently analyzing these features, as well as climate velocity to estimate how far organisms need to move vertically in the water column vs. latitudinally in surface waters to remain within their preferred temperature range. This research is motivated by recently published work by PIs Thorne and Nye (2021) that found that pilot whales have shifted their center of biomass to a much larger degree than their fish and squid prey. This was quite surprising given the large shifts in distribution that have been observed in many species of fish, lobster and crabs. They hypothesized that one reason could be that fish and squid prey can shift their distribution in the water column, but marine mammals are limited by temperatures in the surface waters.

Cetaceans are key predators in marine ecosystems and serve as important sentinels of changes to ocean conditions and food webs (Aguirre and Tabor 2004, Moore 2008, Hazen et al. 2019), and thus understanding changes to cetacean distribution can provide key insights into ecosystem status. An ongoing analysis is assessing how the distribution of odontocetes in the Northeast US has changed relative to changes in water temperature over a 25-year period using records of cetacean stranding events, which can provide important information on cetacean distribution (MacLeod et al. 2005, Evans and Hammond 2004, Pyenson 2011, Thorne and Nye 2021). This analysis suggested that the species composition of odontocetes in the NYB has changed considerably in association with warming waters. In the future, predictions of habitat models of odontocete species and their prey will be used to examine ecosystem implications of changes to the relative distribution of odontocete predators and their prey.

A long-term goal of our work on humpback whale body condition is to link interannual changes in body condition with oceanographic and ecosystem variability, as measured from our

interdisciplinary research cruises on the R/V Seawolf and our glider missions. As we increase our time series in the coming years, we will assess impacts of long-term changes in oceanography and primary and secondary productivity on humpback whale body condition.

Objective 7: Provide supplemental R/V Seawolf vessel staffing support

The hiring freeze instituted by the University in June of 2020 persisted through most of 2021. We were recently given approval to reopen the search, and we have since identified two candidates (both in the process of being hired) for the two vacant full-time deckhand technician positions. Once they are onboarded, we expect to take advantage of the relatively fully staffed vessel operation.

Objective 8: Issues encountered during this period

The major issues encountered for this reporting period are primarily related to ongoing complications due to the SARS-CoV-2 pandemic as well as unforeseen vessel maintenance issues that impacted our summer and fall cruise scheduling. Safety precautions and restrictions on the number of personnel allowed onboard resulted in continued reduced crew operations during our winter and spring monitoring cruises. The limited staffing on the cruises prevented us from conducting any net trawls aboard the R/V Seawolf in 2021.

We have largely avoided supply chain issues by ordering supplies well ahead of time. However, there has been a global shortage of reference material needed to analyze carbonate chemistry samples, so we have spent a significant amount of time making and testing our own reference material. In the long run, this will improve the quality assurance of our analyses, but has delayed the speed with which we can analyze samples. We have also had trouble obtaining reference material for the pH instrument in the lab and thus still have many pH water samples to analyze.

Work planned for upcoming quarters:

Table 5. Activities and deliverables for upcoming quarters.

Objective #	Activity/Deliverable	Timeframe
5	Continue UAV studies of humpback whales	May-Nov. 2022
5	Process UAV imagery and body condition indices, further developing the concept of humpback whale body condition as an ecosystem indicator	Ongoing
5	Obtain UAV imagery of fin whales for body condition studies pending acquisition of appropriate permits	May-Nov. 2022
1-6	Complete four seasonal monitoring cruises including full sampling objectives, adding in seabird line-transect surveys and fish trawls.	Jan. - Dec. 2022
2	Complete three seasonal glider missions	Jan. Dec. 2022
7	Complete hiring of two deckhands	Ongoing
2	Continue processing carbonate chemistry water samples for TA/DIC	Ongoing
3	Continue processing zooplankton samples	Ongoing
1-6	Provide data to the DEC quarterly, or after each monitoring cruise	Jan.-Dec. 2022
2	Purchase a new glider to ensure four deployments while maintaining maintenance schedule	Jan 2022
1-6	Add 6 acoustic moorings to complement Seawolf effort	December 2022
1-6	Modify scope of work and budget	January-March 2022

1-6	Meet with NYSDEC Marine division staff at least 3 times annually	February, March, May 2022
-----	--	---------------------------

References

- Aguirre, A. Alonso, and Gary M. Tabor. 2004. "Introduction: Marine Vertebrates as Sentinels of Marine Ecosystem Health." *EcoHealth* 1 (3): 236–38. <https://doi.org/10.1007/s10393-004-0091-9>.
- Bird, Clara N., and Kc Bierlich. 2020. "CollatriX: A GUI to Collate MorphoMetriX Outputs." *Journal of Open Source Software* 5 (51): 2328. <https://doi.org/10.21105/joss.02328>.
- Brown, Danielle M., Jooke Robbins, Paul L. Sieswerda, Robert Schoelkopf, and E. C. M. Parsons. 2018. "Humpback Whale (*Megaptera Novaeangliae*) Sightings in the New York-New Jersey Harbor Estuary." *Marine Mammal Science* 34 (1): 250–57. <https://doi.org/10.1111/mms.12450>.
- Buckland, Stephen T., David R. Anderson, Kenneth Paul Burnham, Jeffrey Lee Laake, David Louis Borchers, and Leonard Thomas. 2001. "Introduction to Distance Sampling: Estimating Abundance of Biological Populations."
- Christiansen, Fredrik, Antoine M. Dujon, Kate R. Sprogis, John P. Y. Arnould, and Lars Bejder. 2016. "Noninvasive Unmanned Aerial Vehicle Provides Estimates of the Energetic Cost of Reproduction in Humpback Whales." *Ecosphere* 7 (10): e01468. <https://doi.org/10.1002/ecs2.1468>.
- Christiansen, Fredrik, Fabien Vivier, Claire Charlton, Rhianna Ward, Alicia Amerson, Stephen Burnell, and Lars Bejder. 2018. "Maternal Body Size and Condition Determine Calf Growth Rates in Southern Right Whales." *Marine Ecology Progress Series* 592 (March): 267–81. <https://doi.org/10.3354/meps12522>.
- Community, B. O.. 2018. "Blender - a 3D modelling and rendering package. Stichting Blender Foundation, Amsterdam". Retrieved from <http://www.blender.org>
- Evans, Peter G. H., and Philip S. Hammond. 2004. "Monitoring Cetaceans in European Waters." *Mammal Review* 34 (1–2): 131–56. <https://doi.org/10.1046/j.0305-1838.2003.00027.x>.
- Government of Canada, Public Services and Procurement Canada. 2002. "Eastern Canada Seabirds at Sea (ECSAS) Standardized Protocol for Pelagic Seabird Surveys from Moving and Stationary Platforms / [by] Carina Gjerdrum, David A. Fifield, and Sabina I. Wilhelm. : CW69-5/515E-PDF - Government of Canada Publications - Canada.Ca." July 1, 2002. <https://publications.gc.ca/site/eng/389623/publication.html>.

- Groskreutz, Molly J., John W. Durban, Holly Fearnbach, Lance G. Barrett-Lennard, Jared R. Towers, and John K. B. Ford. 2019. “Decadal Changes in Adult Size of Salmon-Eating Killer Whales in the Eastern North Pacific.” *Endangered Species Research* 40 (November): 183–88. <https://doi.org/10.3354/esr00993>.
- Hazen, Elliott L, Briana Abrahms, Stephanie Brodie, Gemma Carroll, Michael G Jacox, Matthew S Savoca, Kylie L Scales, William J Sydeman, and Steven J Bograd. 2019. “Marine Top Predators as Climate and Ecosystem Sentinels.” *Frontiers in Ecology and the Environment* 17 (10): 565–74. <https://doi.org/10.1002/fee.2125>.
- Heim, K.C., Thorne, L.H., Warren, J.D., Link, J.S., Nye, J.A, 2021. Marine ecosystem indicators are sensitive to ecosystem boundaries and spatial scale. *Ecological Indicators*. 125 <https://doi.org/10.1016/j.ecolind.2021.107522>.
- Hirtle, N.O., Stepanuk, J.E.F., Heywood, E.I., Christiansen, F., Thorne, L.H. *In Review*. “Integrating 3D models with morphometric measurements to improve volumetric estimates in large mammals.” *Methods in Ecology and Evolution*.
- Jolly, G. M., and I. Hampton. 2011. “A Stratified Random Transect Design for Acoustic Surveys of Fish Stocks.” *Canadian Journal of Fisheries and Aquatic Sciences*, April. <https://doi.org/10.1139/f90-147>.
- MacLeod, Colin D., Sarah M. Bannon, Graham J. Pierce, Caroline Schweder, Jennifer A. Learmonth, Jerry S. Herman, and Robert J. Reid. 2005. “Climate Change and the Cetacean Community of North-West Scotland.” *Biological Conservation* 124 (4): 477–83. <https://doi.org/10.1016/j.biocon.2005.02.004>.
- Moore, Sue E. 2008. “Marine Mammals as Ecosystem Sentinels.” *Journal of Mammalogy* 89 (3): 534–40. <https://doi.org/10.1644/07-MAMM-S-312R1.1>.
- Pyenson, Nicholas D. 2011. “The High Fidelity of the Cetacean Stranding Record: Insights into Measuring Diversity by Integrating Taphonomy and Macroecology.” *Proceedings of the Royal Society B: Biological Sciences* 278 (1724): 3608–16. <https://doi.org/10.1098/rspb.2011.0441>.
- Stepanuk, Julia E. F., Eleanor I. Heywood, Jennifer F. Lopez, Robert A. DiGiovanni Jr, and Lesley H. Thorne. 2021. “Age-Specific Behavior and Habitat Use in Humpback Whales: Implications for Vessel Strike.” *Marine Ecology Progress Series* 663 (March): 209–22. <https://doi.org/10.3354/meps13638>.

- Thorne, L. H., and J. A. Nye. 2021. “Trait-Mediated Shifts and Climate Velocity Decouple an Endothermic Marine Predator and Its Ectothermic Prey.” *Scientific Reports* 11 (1): 18507. <https://doi.org/10.1038/s41598-021-97318-z>.
- Torres, Walter I., and Kc Bierlich. 2020. “MorphoMetriX: A Photogrammetric Measurement GUI for Morphometric Analysis of Megafauna.” *Journal of Open Source Software* 5 (45): 1825. <https://doi.org/10.21105/joss.01825>.